OPEN ACCESS eBooks

DR. L. RAJENDRAN

PROFESSOR, DEPARTMENT OF MATHEMATICS, AMET UNIVERSITY, CHENNAI

DR. R. SWAMINATHAN

HEAD - DEPARTMENT OF MATHEMATICS,

VIDHYAA GIRI COLLEGE OF ARTS AND SCIENCE, PUDUVAYAL, KARAIKUDI.

Advances in CHEMICAL ENGINEERING

PREFACE

In diverse areas of mathematics, physics, chemistry, and biology, and several applications, nonlinear differential / partial differential equations are included. To proper understanding the qualitative characteristics of many phenomena and processes in various fields of natural science, exact (closed-form) solutions of differential equations play an essential role. Nonlinear systems are complicated because of the high dependency of the system variables on each other. Most of the Engineers are using linear systems or linearization of the nonlinear system in their analysis the nonlinear problems are challenging to solve and are so expensive.

The approximate analytical solutions can serve as a basis for perfecting and testing computer algebra software packages for solving differential equations. It is significant that many equations of physics, chemistry and biology contain empirical parameters. This solutions allow researchers to design and run experiments, by creating appropriate natural conditions, to determine these parameters or functions.This book contains some nonlinear problems in physical and chemical sciences.

A large number of new approximate solutions to nonlinear equations are described. Equations of parabolic, mixed, and general types of first, Second-order nonlinear equations are considered. The nonlinear problem in this book can also apply nonlinear problem in heat and mass transfer, wave theory, nonlinear mechanics, hydrodynamics, gas dynamics, plasticity theory, nonlinear acoustics, combustion theory, nonlinear optics, theoretical physics, differential geometry, control theory, chemical engineering sciences, biology, and other fields.

Therefore, some of the methods are outlined in a schematic and somewhat simplified manner, with necessary references made to books where these methods are considered in more detail. This book may be used by lecturers of universities and colleges for practical courses and lectures on nonlinear mathematical physics for graduate and postgraduate students. Furthermore, the books may be used for researchers in field of modelling of nonlinear processes in physical and chemical sciences.

The authors hope that a broad range of scientists, university professors, engineers, and students in the fields of mathematics, physics, dynamics, power, chemistry, and engineering sciences will benefit from this book.

ACKNOWLEDGEMENTS

The Authors are very grateful to the reviewers with valuable comments and suggestions. I take this opportunity to express my sincere gratitude to Shri J. Ramachandran, Chancellor, for his constant support, encouragement, and the excellent academic and research atmosphere provided.

I wish to thank Col. Dr G. Thiruvasagam, Vice-Chancellor, AMET, University, for his various plans to develop the research activities of hardworking researchers to set new goals in interdisciplinary areas. His sound managerial principles, coupled with his future vision, have been of great help to the mathematics research community.

we express my sincere thanks to Dr M Jayaprakashvel, Registrar, Academy of Maritime Education and Training (AMET), Deemed to be University for his constant support and encouragement. The author is also thankful to Dr D.Rajasekar, professor, Business school, AMET University, for the motivation. Special thanks to **Marwan Abukhaled**, Professor, Department of Mathematics and Statistics, American University of Sharjah, Sharjah, UAE, and Professor Mike Lyons, Professor in Physical Chemistry & Head of School, The University of Dublin, for his valuable suggestions.

It is not out of place to acknowledge the efforts of my PhD scholars who worked with me on my CSIR, UGC and DST-SERB research projects. The research work related to this field has greatly inspired me to write this book.I also express my sincere gratitude to our research scholars M. Chitra Devi, J. Visuvasam, R. JoySalomi, R. Usha Rani, S.Vinolyn Sylvia, B. Manimegalai, for their kind cooperation during the preparation of the book.

I have received considerable assistance from my colleagues Dr P. Balaganesan, Dr I. Paulraj Jayasimman, in the Department of Mathematics, AMET University. Moreover, I am especially grateful to the team of NOVA publishers for cooperation in all aspects of the production of the book.

I thank my parents for their blessings. Last but not least, I thank my wife, SP. Ananthi and my daughters R. Revathy and R. Priyanka for their patience and support. I am looking forward to receiving comments and suggestions on this work from students, teachers, and researchers.

Published in: Jan 2021
Online Edition available at: http://openaccessebooks.com/
Reprints request: info@openaccessebooks.com

Citation: L Rajendran. Non-Linear Problems in Chemical and Physical Sciences. Openaccess eBooks. 2021.

Non-Linear Problems in Chemical and Physical Sciences

Chapter 1

Dr. L. Rajendran[1*]; Dr. R. Swaminathan[2]

[1]Professor, Department of Mathematics, AMET University, Chennai

[2]Head of the Department of Mathematics,, Vidhyaa Giri College of Arts and Science, Karaikudi

Email: raj_sms@rediffmail.com

1. Introduction

1.1. Mathematical Modeling

A mathematical model is a description of a system using mathematical concepts and language. The process of developing a mathematical model is termed mathematical modeling. Mathematical models can take many forms, including but not limited to dynamical systems, statistical models, differential equations, or game theoretic models. These and other types of models can overlap, with a given model involving a variety of abstract structures. In general, mathematical models may include logical models, as far as logic is taken as a part of mathematics. In many cases, the quality of a scientific field depends on how well the mathematical models developed on the theoretical side agree with results of repeatable experiments. Lack of agreement between theoretical mathematical models and experimental measurements often leads to important advances as better theories are developed.

If all the operators in a mathematical model exhibit linearity, the resulting mathematical model is defined as linear. A model is considered to be nonlinear otherwise. The definition of linearity and nonlinearity is dependent on context, and linear models may have nonlinear expressions in them. For example, in a statistical linear model, it is assumed that a relationship is linear in the parameters, but it may be nonlinear in the predictor variables. Similarly, a differential equation is said to be linear if it can be written with linear differential operators, but it can still have nonlinear expressions in it. In a mathematical programming model, if the objective functions and constraints are represented entirely by linear equations, then the model is regarded as a linear model. If one or more of the objective functions or constraints are represented with a nonlinear equation, then the model is known as a nonlinear model.

Nonlinearity, even in fairly simple systems, is often associated with phenomena such as chaos and irreversibility. Although there are exceptions, nonlinear systems and models tend to be more difficult to study than linear ones. A common approach to nonlinear problems is linearization, but this can be problematic if one is trying to study aspects such as irreversibility, which are strongly tied to nonlinearity.

One can think of mathematical modeling as an activity or process that allows a mathematician to be a bio-chemical, an ecologist, an economist, a physiologist. Instead of undertaking experiments in the real world, a modeler undertakes experiments on mathematical representations of the real world. Analytical models are mathematical models that have a closed form solution, i.e. the solution to the differential equations used to describe changes in a system can be expressed as a mathematical analytic function.

1.2. Boundary value problems

In mathematics, in the field of differential equations, a boundary value problem is a differential equation together with a set of additional restraints, called the boundary conditions. A solution to a boundary value problem is a solution to the differential equation which also satisfies the boundary conditions.

Boundary value problems arise in several branches of physics and chemistry. Problems involving the diffusion or heat equation such as the determination of normal modes, are often stated as boundary value problems. A large class of important boundary value problems is the Sturm–Liouville problems. The analysis of these problems involves the eigen functions of a differential operator. To be useful in applications, a boundary value problem should be well posed. This means that given the input to the problem there exists a unique solution, which depends continuously on the input. Much theoretical work in the field of partial differential equations is devoted to proving that boundary value problems arising from scientific and engineering applications are in fact well-posed.

1.3. Biochemical systems

Mathematical modeling in biochemical system is based on ordinary differential equations (ODE) or partial differential equations (PDE). Biochemical processes are represented using power-law expansions in the variables of the system. This framework, which became known as Biochemical systems Theory, has been developed since the 1960s by Michael Savageau and others for the systems analysis of biochemical processes [1,2]. According to Cornish-Bowden they “regarded this as a general theory of metabolic control, which includes both metabolic control analysis and flux-oriented theory as special cases [3]. The dynamics of a species is represented by a differential equation with the structure:

$$\frac{dX_i}{dt} = \sum_j \mu_{ij} \cdot \gamma_j \prod_k X_k^{f_{jk}} \qquad (1.1)$$

Where X_i represents one of the n_d variables of the model (metabolite concentrations, protein concentrations or levels of gene expression). j represents the n_f biochemical processes affecting the dynamics of the species. On the other hand, μ_{ij} (stoichiometric coefficient), γ_j (rate constants) and f_{jk} (kinetic orders) are two different kinds of parameters defining the

dynamics of the system.

The principal difference of power-law modelswith respect to other ODE models used in biochemical systems is that the kinetic orders can be non-integer numbers. A kinetic order can have even negative value when inhibition is modelled. In this way, power-law models have a higher flexibility to reproduce the non-linearity of biochemical systems. Modelling and Simulating networks of biochemical reactions are an active research field today.

In general, using matrix notation, one can always write down the rate laws for a system of biochemical reactions on the following form:

$$N_j = \frac{dS}{dt} \qquad (1.2)$$

Where S is a vector of concentrations, j is a vector of reaction fluxes, and N denotes the stoichiometric matrix. The resulting system of ordinary differential equations can be solved using some suitable numerical or analytical method. In this book some of the following nonlinear bio-chemical problems are solved analytically and numerically.

1.4. Concentrations inside the cationic glucose sensitive membrane

In spite of extensive experimental investigations, only a few studies concerned mathematical modelling of such systems [4-8]. Albin et al. [9] developed a mathematical model to describe the steady state behaviour of a cationic glucose-sensitive membrane. Gough and co-workers [6-8] modelled the steady state behaviour and transient response of a cylindrical glucose sensor. Wuet al. [9] derived a mathematical model with consideration of oxygen limitation to describe the glucose sensitivity of a cationic membrane at the steady state conditions. The reaction scheme in a glucose-sensitive membrane can be written as follows:

$$\text{Glucose} + O_2 \xrightarrow{Glucoseoxidase} \text{Gluconic acid} + H_2O_2 \qquad (1.3)$$

The catalase catalyzes the conversion of hydrogen peroxide to oxygen and water:

$$H_2O_2 \xrightarrow{catalase} H_2O_2 + \frac{1}{2}O_2 \qquad (1.4)$$

If an excess of catalase is immobilized with glucose oxidase, all hydrogen peroxide is reduced. Thus, the overall reaction becomes:

$$\text{Glucose} + O_2/2 \rightarrow \text{Gluconicacid} \qquad (1.5)$$

The corresponding governing system of non-linear differential equation in planar co-ordinates inside the cationic glucose sensitive membrane may be written as [10]:

$$D_{OX}\frac{\partial^2 C_{OX}}{\partial x^2} - \frac{1}{2}\frac{v_{max}C_g C_{OX}}{C_{OX}(k_g + C_g) + C_g k_{OX}} = 0 \qquad (1.6)$$

$$D_a \frac{\partial^2 C_a}{\partial x^2} + \frac{v_{max} C_g C_{OX}}{C_{OX}(k_g + C_g) + C_g k_{OX}} = 0 \quad (1.7)$$

$$D_g \frac{\partial^2 C_g}{\partial x^2} - \frac{v_{max} C_g C_{OX}}{C_{OX}(k_g + C_g) + C_g k_{OX}} = 0 \quad (1.8)$$

Where C_{OX}, C_a and C_a denote the concentration of the oxygen, glucose and gluconic acid respectively. D_g, D_{ox} *and* D_a are the corresponding diffusion coefficients. x is the spatial coordinate and v_{max} is the maximum reaction rate. k_g *and* k_{ox} are Michaelis-Menten constant for the glucose and glucose oxidase respectively? Equations (1.6) - (1.8) are solved for the following boundary conditions by assuming that the membrane is immersed in a well stirred external medium with a constant concentration of each species due to continuous flow of a fresh medium.

$$C_{OX} = C_{OX}^*; \; C_g = C_g^*; \; C_a = 0 \text{ at } x = 0, x = l \quad (1.9)$$

Where l is the thickness of the membrane and C_{OX}^* and C_g^* are the concentrations of oxygen and glucose in the external solution, respectively. In this book, the above problem was solved analytically for all values of the parameters using the Homotopy analysis method.

1.5. Immobilized enzymes system with reversible Michaelis-Menten Kinetics

Recently, there has been much interest in the development of Immobilized enzyme system are immobilized enzyme system are also analyzed for more complex kinetics: reversible reactions [11], competitive Michaelis-Menten kinetics [12] or two-substrate enzymatic reactions [13]. Under these above assumptions, the differential mass balance equation for substrate and product in spherical co-ordinates are a follows [14]:

$$D_S \frac{d^2 C_S}{dr^2} + \frac{2D_S}{r}\left(\frac{dC_S}{dr}\right) = V_S \quad (1.10)$$

$$D_P \frac{d^2 C_P}{dr^2} + \frac{2D_P}{r}\left(\frac{dC_P}{dr}\right) = -V_S \quad (1.11)$$

The boundary conditions are

$$\frac{dC_S}{dr} = 0; \; \frac{dC_P}{dr} = 0 \text{ when } r = 0 \quad (1.12)$$

$$C_S = C_{SR}; C_P = C_{PR} \text{ when } r = R \quad (1.13)$$

Where $V_S = \frac{V_m\left(C_S - \left(C_P / K_{eq}\right)\right)}{K_M + C_S + \left(K_M / K_P\right)C_P}$ and C_S and C_P denote the dimensional substrate and product concentration, r is the radial co-ordinate. The form of V_S determines the mathematical method to solve the above equations and its complexity. Most of the already published articles on enzymatic solution were dealt with non-reversible Michaelis-Menten kinetics [15]. In book the concentrations were determined by solving the above non linear equation using Homotopy

perturbation method.

1.6. Objectives and scope of the present investigation

The objectives of the present investigation are as follows:

➢ To find the analytical expression of concentrations inside the cationic glucose-sensitive membrane by solving the system of non linear equations using Homotopy analysis method.

➢ To derive a general and closed form of an analytical expression pertaining to the substrate concentration profile and effectiveness factor.

➢ To evaluate the approximate solution of non-linear boundary value problems in immobilized glucoamylase kinetics using asymptotic methods.

➢ To get the analytical expression of concentration and effectiveness factor of the reactant inside the catalyst pellets using modified Adomain decomposition method.

1.7. Organization of the books

This book presents the development of mathematical models using Homotopy perturbation method, Homotopy analysis method and Adomian decomposition method are used to predict the theoretical results on solving the system of nonlinear ordinary and partial differential equations. Numerical simulations are also obtained and compared to show the efficiency of the above methods applied.

I. **Chapter one** gives a short introduction to mathematical models, their applications in differential equations and some bio-chemical systems.

II. **Chapter two** provides a mathematical model of a cationic glucose-sensitive membrane. This model involves the system of non-linear steady-state reaction-diffusion equations. Analytical expressions pertaining to concentration of oxygen, glucose and gluconic acid for all values of parameters are presented. Homotopy analysis method is used to evaluate the approximate analytical solutions of the non-linear boundary value problem. Analytical approximation are compared with numerical simulation results.

III. **Chapter three** presents a mathematical model of immobilized enzyme system. The model is based on non-stationary diffusion equation containing a nonlinear term related to reversible Michaelis-Menten kinetics of the enzymatic reaction. He's Homotopy perturbation method is used to solve the non-linear reaction/diffusion equation in immobilized enzymes system. A general and closed form of an analytical expression pertaining to the substrate concentration profile and effectiveness factor are reported for all possible values of parameters.

IV. **Chapter four** focuses on theoretical model to describe the enzyme reaction, mass transfer and heat effects in the calorimetric system. The model is based on non- stationary diffusion equation containing a non-linear term related to immobilize liver esterase by flow calorimetry. The complex numerical methods (Adomian decomposition method, Homotopy analysis and perturbation method) is used to solve the non-linear differential equations Approximate analytical expressions for substrate concentration have been derived for all values of parameters.

In Chapter five, the analytical expression of concentration and effectiveness factor of the reactant inside the catalyst pellets are derived. The approximate analytical expression for the steady state concentration of substrate for all values of parameters γ and β in a packed bed reactor was obtained using the modified Adomian decomposition method.

V. **Chapter six** is the overall conclusion and future enhancements of the book.

1.8. References

1. M. A. Savageau, Biochemical systems analysis: A study of function and design in molecular biology, Reading, MA, Addison–Wesley, 1976.

2. M. A. Savageau, Biochemical systems analysis: I. Some mathematical properties of the rate law for the component enzymatic reactions in: J. Theor. Biol. 25, pp. 365–369, 1969

3. A. Cornish-Bowden, Metabolic control analysis FAQ, website 18, 2007.

4. G. Albin, T. A. Horbet, S. R. Miller and N. L. Ricker, Theoretical and experimental studies of glucose sensitive membranes, Journal of Controlled Release , Vol. 6, No. 1, pp. 267-291, 1987

5. K. Podual, F. J. Doyle III and N. A. Peppas, Dynamic behavior of glucose oxidase-containing microparticles of poly (ethylene glycol)-grafted cationic hydrogels in an environment of changing pH, Biomaterials, Vol. 21, No. 14, pp.1439–1450, 2000.

6. J. K. Leypoldt and D. A. Gough, Model of a two-substrate enzyme electrode for glucose, Analytical Chemistry, Vol. 56, No. 14, pp. 2896–2904, 1984.

7. D. A. Gough, J. Y. Lusisano and P. H. S. Tse, Two-dimensional enzyme electrode sensor for glucose, Analytical Chemistry, Vol. 57, No. 12, pp. 2351–2357, 1985.

8. J. Y. Lusisano and D. A. Gough, Transient response of the two dimensional glucose sensor, Analytical Chemistry, Vol. 60, No. 13, pp. 1272–1281, 1988.

9. G. Albin, T. A. Horbet, S. R. Miller and N. L. Ricker, Theoretical and experimental studies of glucose sensitive membranes, Journal of Controlled Release, Vol. 6, No. 1, pp. 267-291, 1987.

10. M. J. Abdekhodaie and X. Y. Wu, Modeling of a cationic glucose-sensitive membrane with consideration of oxygen limitation, Journal of Controlled Release, Vol. 254, No. 1-2, pp. 119-127, 2005.

11. A. L. Paiva and F. X. Malcata. Reversible reaction and diffusion within a porous catalyst slab, Chem. Eng. Sci., 52 (23), 4429-4432, 1997.

12. G. Xiu, L. Jiang and P. Li, Mass-transfer limitations for immobilized enzyme-catalyzed kinetic resolution of race mate in a batch reactor, Ind. Eng Chem. Res. 39 4054-4062, 2000.

13. J. M. Engasser and P. Hisland, Diffusion effects on the heterogeneous kinetics of two-substrate enzymic reactions, J. Theor. Biol. 77, 427-440, 1979.

14. J. L. Gomez Carrasco, A. Bodalo Santoyo, E. Gomez Gomez, J. Bastida Rodriguez, M. F. Maximo Martin, M. Gomez Gomez, A short recursive procedure for evaluating effectiveness factors for immobilized enzymes with reversible Michaelis-Menten kinetics, Biochem. Eng. J., 39 ,58-65, 2008.

15. A. Bodalo, J. L. Gomez, E. Gomez, J. Bastida, .L. Iborra and A. Manjon, Analysis of diffusion effects on immobilized enzyme on porous supports with reversible Michaelis-Menten kinetics, Enzyme Microb Technol. 8, 433-438, 1986.

Nolinear Nonlinear Problems in the Cationic Glucose-Sensitive Membrane

Chapter 2

2. Analytical Expressions of Concentrations Inside the Cationic Glucose-Sensitive Membrane

2.1. Introduction

Diabetes is a chronic disease with major vascular and de- generative complications. The common treatment for diabetic patients is periodic insulin injection. However, poor control of blood glucose level and poor patient compliance are associated with this method. This approach is a poor approximation of normal physiological insulin secretion. The better ways of insulin administration are being sought. Therefore, there is a need for self-regulated delivery systems [1,2] having the capability of adapting the rate of insulin release in response to changes in glucose concentration in order to keep the blood glucose levels within the normal range.

Various sensing mechanisms, such as competitive binding, substrate-enzyme reaction, pH-dependent polymer erosion or drug solubility, and various types of devices, have been applied to design glucose-sensitive insulin delivery systems [3-6]. Horbett and co-workers [7-10] were the first to investigate systems consisting of immobilized glucose oxidase in a pH responsive polymeric hydrogel, enclosing a saturated insulin solution. In insulin delivery system, some of which consist of immobilized glucose oxidase and catalase in pH responsive polymeric hydrogels. According to the nature of charge present, the pH sensitive hydrogels may be classified as cationic or anionic. Cationic glucose sensitive hydrogels were experimentally studied extensively [10-13].

In spite of extensive experimental investigations, only a few studies concerned modelling or theoretical design of such systems [14-17]. Albin et al. [9] developed a mathematical model to describe the steady state behaviour of a cationic glucose-sensitive membrane. Gough and co- workers [15-17] modeled the steady state behaviour and transient response of a cylindrical glucose sensor. Wu et al. [18] derived a mathematical model with consideration of oxygen limitation to describe the glucose sensitivity of a cationic membrane at the steady state.

To our knowledge, no general analytical expressions for the concentration of oxygen, glucose and gluconic acid inside the cationic glucose-sensitive membrane have been reported for all values of the parameters [18]. The purpose of this chapter is to derive an analytical expression of the steady-state concentration of reactant by solving the non-linear reaction diffusion equation using Homotopy analysis method (HAM).

2.2. Mathematical Formulation of the Problem

The reaction scheme in a glucose-sensitive membrane can be written as follows:

$$\text{Glucose} + \gamma_E \xrightarrow{\text{Glucose oxidase}} \text{Gluconic acid} + H_2O_2 \qquad (2.1)$$

The catalase catalyzes the conversion of hydrogen peroxide to oxygen and water:

$$H_2O_2 \xrightarrow{\text{Catalase}} H_2O_2 + \frac{1}{2}O_2 \qquad (2.2)$$

If an excess of catalase is immobilized with glucose oxidase, all hydrogen peroxide is reduced. Thus, the overall reaction becomes:

$$\text{Glucose} + \frac{1}{2}O_2 \rightarrow \text{Gluconic acid} \qquad (2.3)$$

Glucose and oxygen diffuse from the medium into the membrane and glucose is converted to gluconic acid, causing a pH drop and a consequent change in the permeability of the membrane to solutes. Based on the reaction, only one-half of an oxygen molecule is consumed per molecule of glucose when an excess of catalase is present. The corresponding governing non-linear differential equation in planar co-ordinates inside the cationic glucose sensitive membrane may be written as [18]:

$$D_{OX}\frac{\partial^2 C_{OX}}{\partial x^2} - \frac{1}{2}\frac{v_{max} C_g C_{OX}}{C_{OX}(k_g + C_g) + C_g k_{OX}} = 0 \qquad (2.4)$$

$$D_g\frac{\partial^2 C_g}{\partial x^2} - \frac{v_{max} C_g C_{OX}}{C_{OX}(k_g + C_g) + C_g k_{OX}} = 0 \qquad (2.5)$$

$$D_a\frac{\partial^2 C_a}{\partial x^2} + \frac{v_{max} C_g C_{OX}}{C_{OX}(k_g + C_g) + C_g k_{OX}} = 0 \qquad (2.6)$$

Where C_{OX}, C_g and C_a denote the concentration of the oxygen, glucose and gluconic acid respectively. D_g, D_{ox} and D_a are the corresponding diffusion coefficients. χ is the spatial coordinate and v_{max} is the maximum reaction rate. k_g and k_{ox} are Michaelis-Menten constant for the glucose and glucose oxidase respectively. Equations (2.4) - (2.6) are solved for the following boundary conditions by assuming that the membrane is immersed in a well stirred external medium with a constant concentration of each species due to continuous flow of a fresh medium.

$$C_{OX} = C_{OX}^*;\ C_g = C_g^*;\ \ C_a = 0 \text{ at } x = 0, x = l \qquad (2.7)$$

Where l is the thickness of the membrane and C_{OX}^* and C_g^* are the concentrations of oxygen and glucose in the external solution, respectively. We can assume that the diffusion coefficient of glucose and gluconic acid are equal ($D_g = D_a = D$). We make the non-linear differential equations (2.4)-(2.6) dimensionless form by defining the following dimensionless

equations. (4.4) - (4.6) are reduced to the following dimensionless forms:

$$\chi=\frac{x}{l};\ u=\frac{C_{OX}}{C_{OX}^{*}};\ v=\frac{C_g}{C_g^{*}};\ w=\frac{C_a}{C_a^{*}};\ \alpha=\frac{k_g}{k_{OX}}; \tag{2.8}$$

$$\beta=\frac{C_g^{*}}{k_{OX}};\ \gamma=\frac{C_g^{*}}{C_{OX}^{*}};\ \mu_1=\frac{v_{max}l^2}{Dk_{OX}};\ \mu_2=\frac{v_{max}l^2}{D_{OX}k_{OX}}$$

Equations (2.4) - (2.6) are reduced to the following dimensionless forms:

$$\frac{\partial^2 u}{\partial\chi^2}-\frac{\mu_2}{2}\frac{u}{1+\frac{\alpha u}{\gamma v}+\frac{\beta u}{\gamma}}=0 \tag{2.9}$$

$$\frac{\partial^2 v}{\partial\chi^2}-\frac{\mu_1}{\gamma}\frac{u}{\left(1+\frac{\alpha u}{\gamma v}+\frac{\beta u}{\gamma}\right)}=0 \tag{2.10}$$

$$\frac{\partial^2 w}{\partial\chi^2}-\frac{\mu_1}{\gamma}\frac{u}{\left(1+\frac{\alpha u}{\gamma v}+\frac{\beta u}{\gamma}\right)}=0 \tag{2.11}$$

Where u, v and w represent the dimensionless concentration of oxygen, glucose and gluconic acid. α, β and γ are dimensionless constant. are the Thiele modulus for the oxygen and glucose. Now the boundary conditions reduces to

$$u(\chi)=1;\ \ v(\chi)=1;\ \ w(\chi)=0 \text{ at } \chi=0 \text{ and } \chi=1 \tag{2.12}$$

The dimensionless concentration of oxygen u, glucose v and gluconic acid w are all related processes. On simplifying equations (2.9) and (2.10) we get,

$$\frac{\partial^2}{\partial\chi^2}\left(\frac{2u(\chi)}{\mu_2}-\frac{\gamma v(\chi)}{\mu_1}\right)=0 \tag{2.13}$$

Integrating equation (2.13), using the boundary conditions (equation (2.12)) we get,

$$v(\chi)=1+\frac{2\mu_1\left[u(\chi)-1\right]}{\gamma\,\mu_2} \tag{2.14}$$

On simplifying equations (2.10) and (2.11) we get,

$$\frac{\partial^2(v(\chi)+w(\chi))}{\partial\chi^2}=0 \tag{2.15}$$

Integrating equation (2.15) and using the boundary conditions (equation. (2.12)) we get,

$$v(\chi)+w(\chi)=1 \tag{2.16}$$

So we wish to obtain an analytical expression for the concentration profile $u(x)$ of oxygen. From this concentration profile one can obtain the concentration of glucose $v(x)$ and gluconic acid $w(x)$.

2.3. Approximate analytical solutions

2.3.1 Homotopy analysis method (HAM)

The Homotopy analysis method (HAM) [19–22] is a general analytic approach to get series solutions of various types of non-linear equations. More importantly, this method provides us a simple way to ensure the convergence of solution series. The HAM gives us with great freedom to choose proper base functions to approximate a non-linear problem. Since Liao's book [23] for the Homotopy analysis method was published in 2003, more and more researchers have been successfully applying this method to various non-linear problems [24] in science and engineering. We have solved the non-linear problem using this method. The basic concept of the method is described in Appendix 2.A. Detailed derivation of the dimensionless concentration of oxygen, glucose and gluconic acid are described in Appendix 2.B.

2.3.2. Solution of boundary value problem

Solution of the system of three non-linear differential equations, (Equations (2.9) - (2.11)) with boundary conditions (Equation (2.12)) give a concentration profile of each species within the membrane.

$$u(\chi) = \cosh\left(\sqrt{\mu_2/2}\right)\chi + B\sinh\left(\sqrt{\mu_2/2}\right)\chi + h\left\{\begin{array}{l} M_1\left[2B\sinh\left(\sqrt{2\mu_2}\right)\chi + (1+B^2)\cosh\left(\sqrt{2\mu_2}\right)\chi + 3(B^2-1) + 2(1-2B^2)\cosh\left(\sqrt{\mu_2/2}\right)\chi\right] \\ + M_2\left[\begin{array}{l} B(3+B^2)\sinh\left(3\sqrt{\mu_2/2}\right)\chi + (1+3B^2)\left(\cosh\left(3\sqrt{\mu_2/2}\right)\chi - \cosh\left(\sqrt{\mu_2/2}\right)\chi\right) \\ + 6(1-B^2)\sqrt{2\mu_2}\left\{\sinh\left(\sqrt{\mu_2/2}\right)\chi + B\chi\cosh\left(\sqrt{\mu_2/2}\right)\chi\right\} \end{array}\right] - D\sinh\left(\sqrt{\mu_2/2}\right)\chi \end{array}\right\} \quad (2.17)$$

$$v(\chi) = 1 + \frac{2\mu_1(u(\chi)-1)}{\gamma\mu_2} \quad (2.18)$$

$$w(\chi) = 1 - v(\chi) \quad (2.19)$$

Where ; ; $M_1 = \frac{\gamma\mu_2(\alpha+\beta)-2\beta\mu_1}{6\gamma(\gamma\mu_2-2\mu_1)}$; $M_2 = \frac{\beta\mu_1}{16\gamma(\gamma\mu_2-2\mu_1)}$; $B = \frac{\left(1-\cosh\left(\sqrt{\mu_2/2}\right)\right)}{\sinh\left(\sqrt{\mu_2/2}\right)}$;

$$D=\frac{1}{\sinh\left(\sqrt{\mu_2/2}\right)}\begin{Bmatrix} M_1\left[2B\sinh\left(\sqrt{2\mu_2}\right)+(1+B^2)\cosh\left(\sqrt{2\mu_2}\right)+3(B^2-1)+2(1-2B^2)\cosh\left(\sqrt{\mu_2/2}\right)\right] \\ +M_2\begin{bmatrix} B(3+B^2)\sinh\left(3\sqrt{\mu_2/2}\right)+(1+3B^2)\left(\cosh\left(3\sqrt{\mu_2/2}\right)-\cosh\left(\sqrt{\mu_2/2}\right)\right) \\ +6(1-B^2)\sqrt{2\mu_2}\left\{\sinh\left(\sqrt{\mu_2/2}\right)+B\cosh\left(\sqrt{\mu_2/2}\right)\right\} \end{bmatrix} \end{Bmatrix} \quad (2.20)$$

Here h is the convergence control parameter. Equations (2.17) - (2.19) represent the analytical expression of the concentration of oxygen $u(x)$, glucose $v(x)$ and gluconic acid $w(x)$ respectively.

Here h is the convergence control parameter. Equations (2.17) - (2.19) represent the analytical expression of the concentration of oxygen $u(x)$, glucose $v(x)$ and gluconic acid $w(x)$ respectively.

2.4 Discussion

The non-linear equations (2.9) – (2.11) are also solved by numerical methods using Scilab/Matlab program. The function pdex4 is used for solving the initial-boundary value problems for parabolic-elliptic partial differential equations. The obtained analytical results are compared with the numerical results for various values of α, β, γ, μ_1 and μ_2. All possible numerical values of the dimensionless parameters used in Wu et.al [18] and in this work are given in **(Table 2.1.)**

This numerical solution is compared with our analytical results in figures 2.1-2.3 and Table 2.3. The average relative error between our analytical result (equation 2.17) and the numerical result of oxygen concentration $\in$ is less than 0.8% for various values of μ_1 and μ_2. The experimental value of the parameters α and β are very small. Since the numerical value of γ is 20, the value of M_1 and M_2 becomes very small. In this case the equation. (2.17) becomes

$$u(\chi)\approx\cosh\left(\sqrt{\mu_2/2}\right)\chi+B\sinh\left(\sqrt{\mu_2/2}\right)\chi.$$

(Figure 2.1) presents the analytical and numerical concentration profiles of oxygen u, glucose v and gluconic acid w for the values of the parameters taken in Wu et al [18]. Figures 2.2 and 2.3 illustrate the concentration profiles of oxygen u, glucose v, and gluconic acid w for various values of μ_1 and μ_2. In all the cases the concentration of oxygen $u(x)$, glucose $v(x)$ are decreases and gluconic acid $w(x)$ increases with the increasing value of parameters μ_1 and μ_2. The concentration of oxygen and glucose decreases within the enzyme matrix from both interfaces ($\chi=0$ and $\chi=1$), reaching a minimum value at a distance ($\chi=1$) within the membrane which is determined by the kinetics of the enzyme reaction and the diffusion properties of the reactants. The concentrations of gluconic acid w increases from both interfaces and reaching a maximum value at the middle of the membrane.

Table 2.1: Numerical values for dimensionless parameters used in this work. The fixed values of the dimensional parameters used in Wu et al. [18] are , , , , , and . $k_g = 6.187 \times 10^{-7}\ mol/cm^3$ $C_g^* = 5.5 \times 10^{-6}\ mol/cm^3$ $C_{OX}^* = 0.274 \times 10^{-6}\ mol/cm^3$ $v_{max} = 2150 \times 10^{-9}\ s^{-1} mol/cm^3$ $D_{OX} = 2.29 \times 10^{-5}\ cm^2/sec$ $D = 6.75 \times 10^{-6}\ cm^2/sec$ $l = 10^{-2}$ cm

Parameters	Wu et.al [18	This work		
		Fig.2. 1	Fig.2. 2	Fig.2. 3
$\alpha = \frac{k_g}{k_{OX}}$	8.84x10^{-5}	8.84 x 10^{-5}	0.1	0.1
$\beta = \frac{C_g^*}{k_{OX}}$	7.87x10^{-4}	7.87 x 10^{-5}	0.5	0.5
$\gamma = \frac{C_g^*}{C_{OX}^*}$	20.0	20.07	5	5
$\mu_1 = \frac{v_{max} l^2}{D k_{OX}}$	4.55x10^{-3}	4.5 x 10^{-3}	50	0.1-100
$\mu_2 = \frac{v_{max} l^2}{D_{OX} k_{OX}}$	1.3x10^{-3}	1.3 x 10^{-3}	50	0.1-100

Table 2.2: Comparison of normalized analytical steady-state concentrations of oxygen A (Equation. 3. 17) with the neumerical results for various values of μ_1 and μ_2 and some fixed values of $\alpha = 8084 \times 10\text{-}5$, $\beta = 7074 \times 10\text{-}4$ and $\gamma = 20$ (Here $\eta = -0.01$)

x	$\mu_1 = \mu_2 = 0.01$			$\mu_1 = \mu_2 = 0.1$			$\mu_1 = \mu_2 = 1$			$\mu_1 = \mu_2 = 5$			$\mu_1 = \mu_2 = 10$		
	Equ (2.17	Eq (2.17	Eq (2.17	Equ (2.17	Eq (2.17	Eq (2.17	Eq (2.17	Eq (2.17	Eq (2.17	Eq (2.17	Eq (2.17	Eq (2.17	Eq (2.17	Eq (2.17	Eq (2.17
0	1	1	0	1	1	0	1	1	0	1	1	0	1	1	0
o.2	0.9996	0.9996	0.00	0.9996	0.9996	0.00	0.9618	0.9617	0.01	0.8387	0.8364	0.27	0.7288	0.7223	0.89
0.4	0.9994	0.9994	0.00	0.9994	0.9994	0.00	0.9429	0.9428	0.01	0.7619	0.7586	0.43	0.6056	0.5967	1.47
0.6	0.9994	0.9994	0.00	0.9994	0.9994	0.00	0.9429	0.9428	0.01	0.7619	0.7586	0.43	0.6056	0.5967	1.47
0.8	0.9996	0.9996	0.00	0.9996	0.9996	0.00	0.9618	0.9617	0.01	0.8387	0.8364	0.27	0.7288	0.7223	0.89
1	1	1	0.00	1	1	0.00	1	1	0.00	1	1	0.00	1	1	0.00
	Average deviation 0.00			Average deviation 0.00			Average deviation 0.01			Average deviation 0.23			Average deviation 0.79		

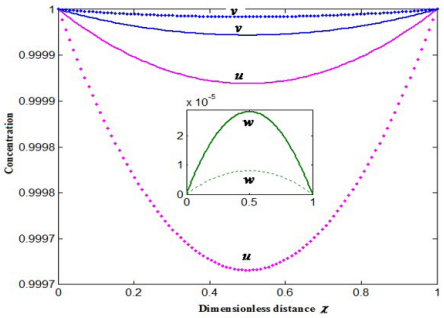

Figures 2.1: Dimensionless concentration profiles of oxygen A and glucose x, against the dimensionless distance x for $\alpha = 8.84 \times 10^{-5}$, $\beta = 7.87 \times 10^{-4}$, $\gamma = 20.07$, $\mu_{1} = 4.55 \times 10^{-3}$, $\mu_{2} = 103 \times 10^{-3}$ *and* $\eta = -0.8$. solid lines present the analytical solution whereas the dotted lines for the numerical solution.

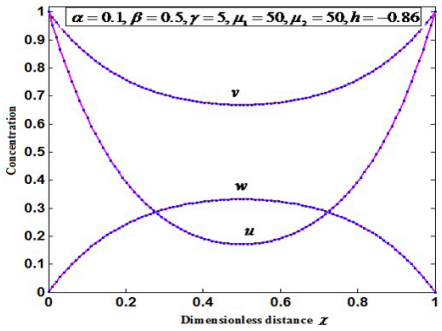

Figures 2.2: Dimensionless concentration profiles of oxygen u, glucose v, and gluconic acid w against the dimensionless distance x for $\alpha = 0.1$, $\beta = 0.5$, $\gamma = 5$, $\mu_{1} = \mu_{2} = 50$ *and* $\eta = -0.86$. Solid lines represent the analytical solution whereas the dotted lines for the numerical solution.

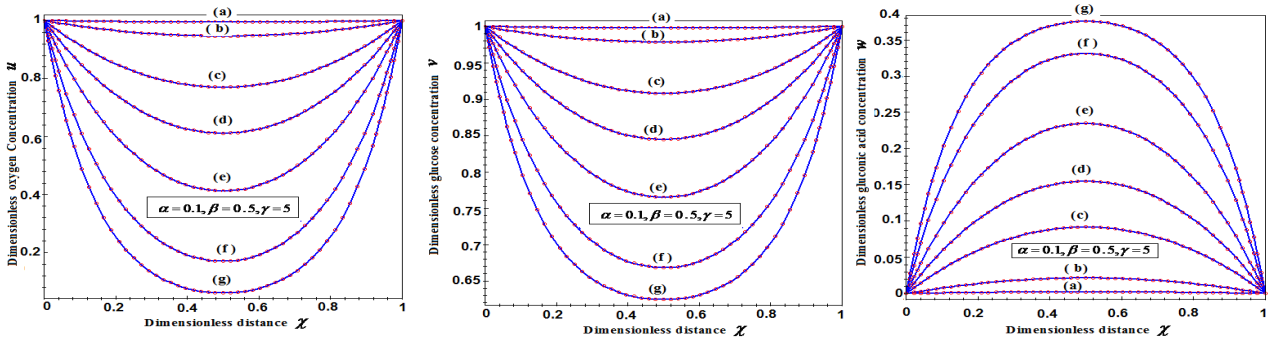

(A) (B) (C)

Figure 2.3: Dimensionless concentration profiles of oxygen u *(A)*, glucose v (B), and gluconic acid w (C) against the dimensionless distance x for (a) $\mu_{1} = \mu_{2} = 0.1$, $\eta = -0.55$ *(b)* $\mu_{1} = \mu_{2} = 1$, $\eta = -0.559$, *(c)* $\mu_{1} = \mu_{2} = 5$, $\eta = -0.62$, *(d)* $\mu 1 = \mu 2 = 10$, $\eta = -0.675$, *(e)* $\mu_{1} = \mu_{2} = 20$, $\eta = -0.74$ *(f)* $\mu_{1} = \mu_{2} = 50$, $\eta = -0.8$ *(g)* $\mu_{1} = \mu_{2 = 100,}$ $\eta = -0.799$.

2.5. Conclusions

A non-linear time independent equation has been solved analytically using homotopy analysis method. The primary result of this work is the first approximate calculations concentrations of oxygen, glucose and gluconic acid for diffusion reaction at the steady state. A simple closed form of analytical expression of concentration of oxygen, glucose and gluconic acid are given in terms of parameters. The analytical results can be used to analyze the effect of different parameters and optimization of the design of glucose membrane.

2.6. Appendix 2.A:

Basic idea of Liao's Homotopy analysis method

Consider the following differential equation [23]:

$$N[u(\chi)]=0 \tag{2.A1}$$

Where, N is a nonlinear operator, x denotes an independent variable, $u(x)$ is an unknown function. For simplicity, we ignore all boundary or initial conditions, which can be treated in the similar way. By means of generalizing the conventional homotopy method, Liao constructed the so-called zero-order deformation equation as:

$$(1-p)L[\varphi(\chi;p)-u_0(\chi)]=phH(\chi)N[\varphi(\chi;p)] \tag{2.A2}$$

Where $p\in[0,1]$ is the embedding parameter, $h\neq 0$ is a nonzero auxiliary parameter, $H(\chi)\neq 0$ is an auxiliary function, L is an auxiliary linear operator, $u_0(\chi)$ is an initial guess of $u(\chi)$ and $\varphi_{\varphi(\chi:p)}$ is an unknown function. It is important, that one has great freedom to choose auxiliary unknowns in HAM. Obviously, when $p=0$ and $p=1$, it holds:

$$\varphi(\chi;0)=u_0(\chi) \text{ and } \varphi(\chi;1)=u(\chi) \tag{2.A3}$$

respectively. Thus, as p increases from 0 to 1, the solution $\varphi(\chi;p)$ varies from the initial guess $u_0(\chi)$ to the solution $u(_2)$. Expanding $\varphi(\chi;p)$ in Taylor series with respect to p, we have:

$$\varphi(\chi;p)=u_0(\chi)+\sum_{m=1}^{+\infty}u_m(\chi)p^m \tag{2.A4}$$

where

$$u_m(\chi)=\frac{1}{m!}\frac{\partial^m\varphi(\chi;p)}{\partial p^m}|_{p=0} \tag{2.A5}$$

If the auxiliary linear operator, the initial guess, the auxiliary parameter h, and the auxiliary function are so properly chosen, the series (2.A4) converges at $p = 1$ then we have:

$$u(\chi)=u_0(\chi)+\sum_{m=1}^{\infty}u_m(\chi)\,. \tag{2.A6}$$

Define the vector

$$\vec{u}_n=\{u_0,u_1,...,u_n\} \tag{2.A7}$$

Differentiating equation (2.A2) for m times with respect to the embedding parameter p, and then setting $p = 0$ and finally dividing them by $m!$, we will have the so-called m^{th}-order deformation equation as:

$$L[u_m - \chi_m u_{m-1}] = hH(\chi)\Re_m(\vec{u}_{m-1}) \tag{2.A8}$$

where

$$\Re_m(\vec{u}_{m-1}) = \frac{1}{(m-1)!}\frac{\partial^{m-1}N[\varphi(\chi;p)]}{\partial p^{m-1}}\bigg|_{p=0} \tag{2.A9}$$

and

$$\chi_m = \begin{cases} 0, & m \le 1, \\ 1, & m > 1. \end{cases} \tag{2.A10}$$

Applying L^{-1} on both side of equation (2.A8), we get

$$u_m(\chi) = \chi_m u_{m-1}(\chi) + hL^{-1}[H(\chi)\Re_m(\vec{u}_{m-1})] \tag{2.A11}$$

In this way, it is easily to obtain u_m for $m \ge 1$, at M^{th} order, we have

$$u(\chi) = \sum_{m=0}^{M} u_m(\chi)$$

When $M \to +\infty$, we get an accurate approximation of the original equation (2.A1). For the convergence of the above method we refer the reader to Liao [25]. If equation (2.A1) admits unique solution, then this method will produce the unique solution. If equation (2.A1) does not possess unique solution, the HAM will give a solution among many other (possible) solutions.

2.7 Appendix 2.B:

Approximate analytical solutions of the equation (2.9)

Substituting equation (2.14) in equation. (2.9) and simplifying we get,

$$\frac{\partial^2 u}{\partial \chi^2} - \frac{\mu_2}{2}u + \frac{u}{\gamma(\gamma\mu_2 - 2\mu_1)}\left[\{\mu_2(\alpha+\gamma\beta) + 2\mu_1(\gamma-\beta)\}\frac{\partial^2 u}{\partial \chi^2} - \gamma\mu_1\mu_2 u + 2\beta\mu_1 u\frac{\partial^2 u}{\partial \chi^2}\right] = 0 \tag{2.B1}$$

In order to solve equation (2.B1) by means of the HAM, we first construct the zeroth-order deformation equation by taking $H(\chi) = 1$,

$$(1-p)\left(\frac{\partial^2\varphi}{\partial\chi^2} - \frac{\mu_2}{2}\varphi\right) = ph\left[\begin{array}{l} \dfrac{\partial^2\varphi}{\partial\chi^2} - \dfrac{\mu_2}{2}\varphi + \varphi/\gamma(\gamma\mu_2 - 2\mu_1) \\ \left(\{\mu_2(\alpha+\gamma\beta) + 2\mu_1(\gamma-\beta)\}\dfrac{\partial^2\varphi}{\partial\chi^2} - \gamma\mu_1\mu_2\varphi + 2\beta\mu_1\varphi\dfrac{\partial^2\varphi}{\partial\chi^2}\right) \end{array}\right] \tag{2.B2}$$

where $p \in [0,1]$ is an embedding parameter. When $p = 0$, the above equation becomes,

$$\frac{\partial^2\varphi_0}{\partial\chi^2} - \frac{\mu_2}{2}\varphi_0 = 0 \tag{2.B3}$$

Solving equation. (2.B3) and using the boundary condition

$$\varphi_0(0;p) = 1 \text{ and } \varphi_0(1;p) = 1 \tag{2.B4}$$

we get

$$\varphi_0(\chi) = \cosh\left(\sqrt{\mu_2/2}\right)\chi + B\sinh\left(\sqrt{\mu_2/2}\right)\chi \tag{2.B5}$$

where $B = \dfrac{\left[1-\cosh\left(\sqrt{\mu_2/2}\right)\right]}{\sinh\left(\sqrt{\mu_2/2}\right)}$

When $p=1$ the equation. (2.B2) is equivalent to equation. (2.B1), thus it holds.

$$\varphi(\chi;1) = u(\chi) \tag{2.B6}$$

Expanding $\varphi(\chi;p)$ in Taylor series with respect to the embedding parameter *p*, we have,

$$\varphi(\chi;p) = u_0(\chi) + \sum_{m=1}^{\infty} u_m(\chi)p^m \tag{2.B7}$$

where $u_0(\chi) = u(\chi;0)$ (2.B8)

$$u_m(\chi) = \frac{1}{m!}\frac{\partial^m u(\chi;p)}{\partial p^m}\bigg|_{p=0} \tag{2.B9}$$

and $u_m(\chi)$ $[m=1,2,...]$ will be determined later. Note that the above series contains the convergence control parameter *h*. Assuming that *h* is chosen so properly that the above series is convergent at $p=1$. We have the solution series as

$$u(\chi) = \varphi(\chi;1) = u_0(\chi) + \sum_{m=1}^{\infty} u_m(\chi) \tag{2.B10}$$

Substituting (2.B10) into the zeroth-order deformation equations (2.B7) and (2.B8) equating the co-efficient of *p* we have,

$$\frac{\partial^2\varphi_1}{\partial\chi^2} - \frac{\mu_2}{2}\varphi_1 - h\varphi/\gamma(\mu_2 - 2\mu_1)\left(\{\mu_2(\alpha+\beta) + 2\mu_1(\gamma-\beta)\}\frac{\partial^2\varphi}{\partial\chi^2} - \mu_1\mu_2\varphi + 2\beta_1\varphi\frac{\partial^2\varphi}{\partial\chi^2}\right) = 0 \tag{2.B11}$$

Solving equation (2.B11) and using the boundary conditions $\varphi_1(0) = 0,$ and $\varphi_1(1) = 0$, we get

$$\varphi_1(\chi) = h\left\{\begin{array}{l} M_1\left[\begin{array}{l} 2B\sinh\left(\sqrt{2\mu_2}\right)\chi + (1+B^2)\cosh\left(\sqrt{2\mu_2}\right)\chi \\ +3(B^2-1) + 2(1-2B^2)\cosh\left(\sqrt{\mu_2/2}\right)\chi \end{array}\right] \\ +M_2\left[\begin{array}{l} B(3+B^2)\sinh\left(3\sqrt{\mu_2/2}\right)\chi + (1+3B^2)\left\{\begin{array}{l}\cosh\left(3\sqrt{\mu_2/2}\right)\chi \\ -\cosh\left(\sqrt{\mu_2/2}\right)\chi\end{array}\right\} \\ +6(1-B^2)\sqrt{2\mu_2}\left\{\sinh\left(\sqrt{\mu_2/2}\right)\chi + B\chi\cosh\left(\sqrt{\mu_2/2}\right)\chi\right\}\end{array}\right] \\ -D\sinh\left(\sqrt{\mu_2/2}\right)\chi \end{array}\right\} \tag{2.B12}$$

Adding equations (2.B5) and (2.B12) we obtain the final results as described in equation (2.17) in the text.

2.8 Appendix 2.C:

Scilab / Matlab program

A SCILAB/MATLAB program for the numerical solution of the system of non-linear second order differential equations (2.9)-(2.11)

```
function pdex4
m = 0;
x=linspace(0,1);
t=linspace(0,100000);
sol=pdepe(m,@pdex4pde,@pdex4ic,@pdex4bc,x,t);
u1=sol(:,:,1);
u2=sol(:,:,2);
u3=sol(:,:,3);
figure
plot(x,u1(end,:))
title(‚u1 (x,t)‘)
xlabel(‚Distance x‘)
ylabel(‚u1 (x,2)‘)
%---------------------------------------------------------------------
figure
plot(x,u2(end,:))
title(‚u2 (x,t)‘)
xlabel(‚Distance x‘)
ylabel(‚u2 (x,2)‘)
% ------------------------------------------------------------
figure
plot(x,u3(end,:))
title(‚u3 (x,t)‘)
xlabel(‚Distance x‘)
ylabel(‚u3 (x,2)‘)
% ------------------------------------------------------------
function [c,f,s] = pdex4pde(x,t,u,DuDx)
c = [1; 1; 1];
f = [1; 1; 1] .* DuDx;
a=0.5;
b=5;
y=5;
u2=0.1;
u1=5;
```

```
F=-u2*u (1)/(2*(a/y*u(1)/u(2)+b/y*u(1)+1));
F1=-u1*u (1)/(y*(a/y*u(1)/u(2)+b/y*u(1)+1));

F2=u1*u (1)/(y*(a/y*u(1)/u(2)+b/y*u(1)+1));
s=[F; F1; F2];
% --------------------------------------------------------------
function u0 = pdex4ic(x);
u0 = [0; 1; 0];
% --------------------------------------------------------------
function [pl,ql,pr,qr]=pdex4bc(xl,ul,xr,ur,t)
pl = [ul(1)-1; ul(2)-1; ul(3)];
ql = [0; 0; 0];
pr = [ur(1)-1; ur(2)-1; ur(3)];
qr = [0; 0; 0];
```

2.9. References

1. K. Park, Nanotechnology: What it can do for drug delivery, Journal of Controlled Release, Vol. 120, No. 1-2, pp. 1-3, 2007.

2. J. Kost and R. Langer, Responsive polymer systems for controlled delivery of Therapeutics, Trends in Biotechnology, Vol. 10, pp. 127-131, 1992.

3. L. A. Klumb and T. A. Horbett, Design of insulin delivery devices based on glucose sensitive membranes, Journal of Controlled Release, Vol. 18, No. 1, pp. 59-80, 1992.

4. J. Kost and R. Langer, Responsive polymeric delivery systems, Advanced Drug Delivery Reviews, Vol. 46, No. 1, pp. 125-148, 2001.

5. S. W. Kim and H. A. Jacobs, Self-regulated insulin delivery-artificial pancreas, Drug Development and Industrial Pharmacy, Vol. 20, No. 4, pp.575–580, 1994.

6. S. J. Lee and K. Park, Glucose-sensitive phase-reversible hydrogels, in: R.M. Ottenbrite, S.J. Huang, K. Park (Eds.), Hydrogels and Biodegradable Polymers for Bioapplications, ACS, Washington, DC, Chapter 2, pp. 11–16, 1996.

7. J. Kost, T. A. Horbett, B. D. Ratner and M. Singh, Glucose-sensitive membranes containing glucose oxidase: activity, swelling, and permeability studies, Journal of Biomedical Materials Research, Vol. 19, No. 9, pp. 1117-1133, 1985.

8. G. Albin, T. A. Horbet and B. D. Ratner, Glucose-sensitive membranes for controlled delivery of insulin: insulin transport studies, Journal of Controlled Release, Vol. 3, pp. 153-164, 1985.

9. G. Albin, T. A. Horbet, S. R. Miller and N. L. Ricker, Theoretical and experimental studies of glucose sensitive membranes, Journal of Controlled Release, Vol. 6, No. 1, pp. 267-291, 1987.

10. G. Albin, T. A. Horbett and B. D. Ratner, Gulcose-sensitive membranes for controlled delivery of insulin, In: Kost J, Editor. Pulsed and self-regulated drug delivery. Boca Raton, FL: CRC Press, p. 159-185, 1990.

11. T. Traitel, Y. Cohen and J. Kost, Characterization of a glucose sensitive insulin release system in simulated in vivo conditions, Biomaterials, Vol. 21, No. 16, pp.1679– 1687, 2000.

12. M. Glodrich and J. Kost, Glucose sensitive polymeric matrices for controlled drug delivery, Clinical Materials,

Vol.13, No.1-4, pp. 135–142, 1993.

13. K. Podual, F. J. Doyle III and N. A. Peppas, Glucose sensitivity of glucose oxidase containing cationic copolymer hydrogels having poly(ethylene glycol) grafts, Journal of Controlled Release, Vol. 67, No. 1, pp. 9-17, 2000.

14. K. Podual, F. J. Doyle III and N. A. Peppas, Dynamic behavior of glucose oxidase-containing microparticles of poly (ethylene glycol)-grafted cationic hydrogels in an environment of changing pH, Biomaterials, Vol. 21, No. 14, pp.1439–1450, 2000.

15. J. K. Leypoldt and D. A. Gough, Model of a two-substrate enzyme electrode for glucose, Analytical Chemistry, Vol. 56, No. 14, pp. 2896–2904, 1984.

16. D. A. Gough, J. Y. Lusisano and P. H. S. Tse, Two-dimensional enzyme electrode sensor for glucose, Analytical Chemistry, Vol. 57, No. 12, pp. 2351–2357. J. Y.

a. Lusisano and D. A. Gough, Transient response of the two dimensional glucose sensor, Analytical Chemistry, Vol. 60, No. 13, pp. 1272–1281, 1985.

17. J. Y. Lusisano and D. A. Gough, Transient response of the two dimensional glucose sensor, Analytical Chemistry, Vol. 60, No. 13, pp. 1272–1281, 1988.

18. M. J. Abdekhodaie and X. Y. Wu, Modeling of a cationic glucose-sensitive membrane with consideration of oxygen limitation, Journal of Membrane Science, Vol. 254, No. 1- 2, pp. 119-127, 2005.

19. S. J. Liao, The proposed homotopy analysis technique for the solution of nonlinear problems, PhD thesis, Shanghai Jiao Tong University, 1992.

20. S. J. Liao, On the homotopy analysis method for nonlinear problems, Applied Mathematics and Computation Vol.147, No.2, pp. 499-513, 2004.

21. S. J. Laio, Notes on the homotopy analysis method: some definitions and theorems, Communications in Nonlinear Science and Numerical Simulation, Vol. 14, No. 4, pp. 983-997, 2009.

22. S. J. Liao and Y. Tan, A general approach to obtain series solutions of nonlinear differential equations, Studies in Applied Mathematics, Vol. 119, No. 4, pp.297-355, 2007.

23. S. J. Liao, Beyond Perturbation: Introduction to the homotopy analysis method, 1st Edition, Chapman and Hall, CRC Press, Boca Raton, p: 336, 2003.

24. S. Loghambal and L. Rajendran, Analytical expressions of concentration of nitrate pertaining to the electrocatalytic reduction of nitrate ion, Journal of Electroanalytical Chemistry, Vol. 661, No. 1, 2011, pp. 137–143, 2011.

25. G. Domairry and M. Fazeli, Homotopy analysis method to determine the fin efficiency of convective straight fins with temperature-dependent thermal conductivity, Communications in Nonlinear Science and Numerical Simulation, Vol.14, No.2 , pp.489-499, 2009.

Boundary Vale Problems and Immobilized Enzymes with Reversible Michaelis Menten Kinetics

Chapter 3

3.1. Introduction

Immobilization of enzymes helps in their economic reuse and in the development of continuous bioprocesses. Enzymes can be immobilized either using the isolated enzymes or the whole cells. Immobilization often stabilizes structure of the enzymes, thereby allowing their applications even under harsh environmental conditions of pH, temperature and organic solvents, and thus enables their uses at high temperatures in nonaqueous enzymology, and in the fabrication of biosensor probes. In the future, development of techniques for the immobilization of multienzymes along with cofactor regeneration and retention system can be gainfully exploited in developing biochemical processes involving complex chemical conversions.

The internal diffusional effects can be quantitatively expressed by the effectiveness factor η. The effectiveness factor is defined as the ratio of the actual reaction rate inside the particle to the rate in the absence of diffusional limitations [1]. The analytical solution for first-order kinetics, which provides the effectiveness factor value as a hyperbolic function of the Thiele modulus, is well known. For simple Michaelis-Menten kineties, a two-parameter model providing generalized plots of the effectiveness factor as a function of the dimensionless moduli [2, 3]. Immobilized enzyme systems are also analyzed for more complex kinetics: reversible reactions [4], competitive Michaelis-Menten kinetics [5] or two-substrate enzymatic reactions [6].

Analytical solutions have been obtained in the limiting cases of zero and first reaction order [7]. For the remaining, numerical calculus has been ordinarily used, being the different variables of the system expressed in dimensionless form [8-15]. But, since the calculus complexity increases as the reaction mechanism becomes more complex. When reversible or product competitive inhibition mechanisms have been considered, only external diffusional limitations [16] have been evaluated, otherwise unsatisfactory results were obtained [17-19].

Most theoretical models developed for estimating the effectiveness factor for heterogeneous enzymatic systems are based on the following assumptions: The catalytic particle is a porous sphere with a radius R. The enzyme is uniformly distributed throughout the whole catalytic particle. Diffusion reaction takes place at a constant temperature and under steady-state conditions. The substrate and product diffusion inside the catalytic particle can be modeled by Fick's first law and effective diffusivity is the same throughout the particle. The enzymatic reaction is monosubstrate and yields only one product.

Most previously published enzymatic kinetic models involve non-reversible Michaelis -Menten kinetics, and are solved by numerical calculus. Among these models, some of the most relevant are those proposed by Engasser and Horvath [2], for a simple Michaelis-Menten kinetics, modified by Tuncel [3]; The solution developed by Xiu et al. [5] for product competitive inhibition kinetics; or the two-substrate model invented by [6]. The first model has been successfully applied in the design of heterogeneous enzymatic reactors: fixed bed reactors [20], continuous tank reactors [21] and fluidized bed reactors [22]. Recently the methodology used in these papers has been applied to the simulation of a packed bed immobilized enzyme reactor [23,24].

However, approximate analytical solutions, valid only in a limited range of the parameters, have also been published [25-27]. Several numerical methods have been used to solve the boundary value problems outlined in equation (3.1) and (3.2). The most frequently used are finite differences [28] and orthogonal collocation [29], which transforms the problem into a system of algebraic equations. Recently, Chen et al. [30, 31] developed the two-dimensional flow model, incorporating mass transport to simulate a microchannel enzyme reactor with a porous wall using finite volume method. However, to the best of our knowledge, there was no rigorous solution for the substrate concentration has been reported. The purpose of this chapter is to derive simple analytical expression for concentration and effectiveness factor for all possible values of reaction/diffusion parameters ϕ and α.

3.2. Mathematical formulation of the problem and analysis

The mathematical models for estimating the effectiveness factor in heterogeneous enzymatic systems are based on the following assumptions: (i) The catalytic particle is spherical and its radius is R. (ii) The enzyme is uniformly distributed throughout the whole catalytic particle. (iii) The system is in a steady-state and isothermal. Under these above assumptions, the differential mass balance equation for substrate and product in spherical co-ordinates are as follows [33]:

$$D_S \frac{d^2 C_S}{dr^2} + \frac{2D_S}{r}\left(\frac{dC_S}{dr}\right) = V_S \tag{3.1}$$

$$D_P \frac{d^2 C_P}{dr^2} + \frac{2D_P}{r}\left(\frac{dC_P}{dr}\right) = -V_S \tag{3.2}$$

The boundary conditions are

$$\frac{dC_S}{dr} = 0;\ \frac{dC_P}{dr} = 0 \text{ when } r = 0 \tag{3.3}$$

$$C_S = C_{SR}; C_P = C_{PR} \text{ when } r = R \tag{3.4}$$

$$\text{where } V_S = \frac{V_m\left(C_S - \left(C_P / K_{eq}\right)\right)}{K_M + C_S + \left(K_M / K_P\right)C_P} \tag{3.5}$$

and C_S and C_S denote the dimensional substrate and product concentration, *r* is the radial co-ordinate. The form of V_S determines the mathematical method to solve the above equations and its complexity. Most of the already published articles on enzymatic solution were dealt with non-reversible Michaelis-Menten kinetics. The present model is an improvement based on the previously formulated three parameter model [32], since only two parameters are necessary to reach the solution. Adding equations (3.1) and (3.2) and using the boundary conditions the following relationship can be established:

$$C_P = C_{PR} + \frac{D_S}{D_P}\left(C_{SR} - C_S\right) \tag{3.6}$$

Substituting the value of C_P , we can obtain

$$V_S = \frac{V_m\left(1+\frac{1}{K_{eq}}\frac{D_S}{D_P}\right)\left(C_S - C_{SE}\right)}{K_M + \frac{K_M}{K_P}C_{PE} + C_{SE} + \left(1-\frac{K_M}{K_P}\frac{D_S}{D_P}\right)\left(C_S - C_{SE}\right)} \tag{3.7}$$

where

$$K_{eq} = \frac{C_{PE}}{C_{SE}}\ ,\ C_{SE} = \frac{C_{PR} + \left(D_S/D_P\right)C_{PR}}{K_{eq} + \left(D_S/D_P\right)} \text{ and } C_{PE} = K_{eq}C_{SE} = \frac{C_{PR} + \left(D_S/D_P\right)C_{PR}}{1 + \left(1/K_{eq}\right)\left(D_S/D_P\right)}. \tag{3.8}$$

Where C_{SE} and C_{PE} are the equilibrium substrate and product concentration. We make the non-linear differential equations outlined in equation (3.1) and (3.2) in dimensionless form by introducing the following dimensionless parameters:

$$S = \frac{C_S - C_{SE}}{C_{SR} - C_{SE}},\ \rho = \frac{r}{R},\ \varphi = \frac{R^2 V_m}{\left(C_{SR} - C_{SE}\right)D_S}\frac{\left(1+\frac{1}{K_{eq}}\frac{D_S}{D_P}\right)}{\left(1-\frac{K_M}{K_P}\frac{D_S}{D_P}\right)} \text{ and } \alpha = \frac{K_M + \frac{K_M}{K_P}C_{PE} + C_{SE}}{\left(C_{SR} - C_{SE}\right)\left(1-\frac{K_M}{K_P}\frac{D_S}{D_P}\right)} \tag{3.9}$$

The mass balance differential equation for substrate in spherical co-ordinates for two parameter model is [33]:

$$\frac{d^2S}{d\rho^2} + \frac{2}{\rho}\left(\frac{dS}{d\rho}\right) - \phi\frac{S}{\alpha + S} = 0 \tag{3.10}$$

where S is the substrate concentration and ρ is the dimensionless particle radial coordinate and ϕ and α are the dimensionless modules. The boundary conditions are represented as follows:

$$\frac{dS}{d\rho} = 0 \text{ when } \rho = 0 \tag{3.11}$$

$$S = 1 \text{ when } \rho = 1 \tag{3.12}$$

The effectiveness factor can be evaluated as [33]:

$$\eta = 3(\alpha+1)\int_0^1 \frac{S}{\alpha + S}\rho^2 d\rho \tag{3.13}$$

3.3. General result for concentration S and effectiveness factor η

The Homotopy perturbation method [34-40] is used to give the approximate analytical solution of non-linear reaction/diffusion equation (3.10). Using this method (see Appendix –3.A, 3.B and 3.C) we can obtain the concentration of substrate as follows:

$$S(\rho) = 1 + \frac{7\phi^2}{360\alpha^2}\left(1 - \frac{1}{\alpha}\right) - \frac{\phi}{6\alpha} + \left(\frac{\phi}{6\alpha} - \frac{\phi^2}{36\alpha^2} + \frac{\phi^2}{36\alpha^3}\right)\rho^2 + \left(\frac{\phi^2}{120\alpha^2} - \frac{\phi^2}{120\alpha^3}\right)\rho^4 \qquad (3.14)$$

The equation (3.14) satisfies the boundary conditions (3.11) and (3.12). This equation represents the analytical expression of concentration provided $\frac{7\phi^2}{360\alpha^2}\left(1-\frac{1}{\alpha}\right)-\frac{\phi}{6\alpha}<1$. Using equations (3.11) and (3.12), the effectiveness response is given by

$$\eta = \frac{(\alpha+1)}{\phi A}\left[\phi A - 18\alpha^2 A + \arctan\left(\frac{\phi}{A}\right)\left(108\alpha^3(\alpha+1) - 18\alpha^2\phi\right)\right] \qquad (3.15)$$

where

$$A = \sqrt{\phi\left(6\alpha^2 + 6\alpha - \phi\right)} \qquad (3.16)$$

equation. (3.13) represents the new approximate analytical expression for the effectiveness factor for all values of parameter α and ϕ provided $A \neq 0$ and $\frac{7\phi^2}{360\alpha^2}\left(1-\frac{1}{\alpha}\right)-\frac{\phi}{6\alpha}<1$.

3.4. Numerical simulation

The non-linear differential equation (3.10) is solved by numerical methods. The function pdex4 in SCILAB software which is a function of solving the boundary value problems for ordinary differential equation is used to solve this equation. Its numerical solution is compared with Homotopy perturbation method in figures and it gives a satisfactory result when α ≥10.

3.5. Discussion

3.5.1. Effect of Thiele modulus ϕ in concentration of substrate

The Thiele modulus ϕ can be varied by changing either the particle radius or the amount of concentration of substrate. This parameter describes the relative importance of diffusion and reaction in the particle radius. When ϕ is small, the kinetics are the determining factor; the overall uptake of substrate in the enzyme matrix is kinetically controlled. Under these conditions, the substrate concentration profile across the membrane is essentially uniform. In contrast, when the Thiele modulus is large, diffusion limitations are the principal determining factor.

(Figures 3.1 – 3.2) show the dimensionless steady-state substrate concentration for the different values of ϕ calculated using equation (3.12). From these figures, we can see that the value of the concentration increases when ϕ decreases. The concentration of substrate *S*

increases slowly and rises abruptly when and all values of ϕ. When $\phi < 1$ and $\alpha \leq 5$, the concentration of substrate $S \approx 1$ (steady-state value). The simulation result is compared with our simple closed analytical expression equation (3.14), in Tables 3.1. The average relative difference between our equation (3.14) and the simulation result is less than 0.5 % when $\alpha = 2$.

3.5.2. Effect of dimensionless module α in concentration

The dimensionless module α is parameter quantifying the degree of unsaturation/saturation of the catalytic kinetics since it describes the ratio of the substrate concentration within the film to Michaelis –Menten constant. When $\alpha << 1$, and so the kinetics are unsaturated (first order with respect to substrate concentration S). Alternatively, when $\alpha << 1$, and the catalytic kinetics are saturated (zero order with respect to substrate concentration S). Figures 3.3 to 3.4 show the dimensionless steady-state substrate concentration for the different values of α. From these figures, we can see that the value of the concentration increases when α increases for all values of ϕ.

3.5.3. Effectiveness factor η

Effectiveness is an important concept in immobilized enzyme system. Figures 3.5 represents the effectiveness factor η versus dimensionless module η for different values of dimensionless module α. From this figure, it is inferred that, a constant value of dimensionless module α, the effectiveness factor η decreases quite rapidly as dimensionless module ϕ increases, approaching zero at high ϕ values, which corresponds to internal diffusion controlled processes. Moreover, it is also well known that, a constant value of dimensionless module ϕ, the effectiveness factor η increases with increasing values of α.

Table 3.1: Comparison of concentration profile of substrate A for various values of ϕ using equations (14) and simulation result when dimensionless module ($\alpha = 2$).

ρ	Concentration of S								
	A (when $\phi = 0.1$)			S (when $\phi = 5$)			S (when $\phi = 20$)		
	Simulation	This work Eq. (3.14)	% of deviation	Simulation	This work Eq. (3.14)	% of deviation	Simulation	This work Eq. (3.14)	% of deviation
0	0.9900	0.9917	0.1714	0.6452	0.6441	0.0912	0.3051	0.3056	0.1636
0.2	0.9915	0.9920	0.0504	0.6570	0.6576	0.0912	0.3173	0.3176	0.0945
0.4	0.9935	0.9950	0.1508	0.6980	0.6986	0.0859	0.3600	0.3621	0.5799
0.6	0.9955	0.9958	0.0301	0.7679	0.7688	0.1171	0.4561	0.4568	0.1532
0.8	0.9968	0.9970	0.0201	0.8641	0.8647	0.0694	0.6514	0.6646	1.9862
1	1.0000	1.0000	0.0000	1.0000	1.0000	0.0000	1.0000	1.0000	0.0000
	Average		0.0705	Average		0.0758	Average		0.4962

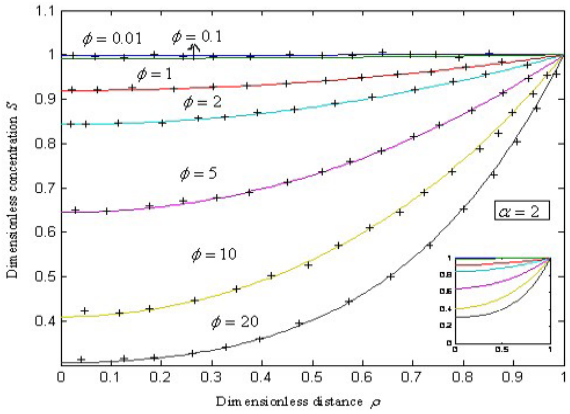

Figure 3.1: Influence of dimensionless module ϕ on the concentration profile of substrate S obtained from our approximate solution presented in this work (equation (3.14), solid line) and from the simulation result (plus line). The plot was constructed for $\alpha = 2$.

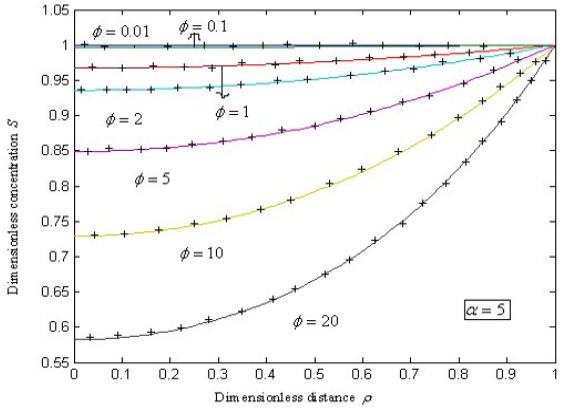

Figure 3.2: Influence of dimensionless module ϕ on the concentration profile of substrate S obtained from our approximate solution presented in this work (equation (3.14), solid line) and from the simulation result (plus line). The plot was constructed for $\alpha = 5$.

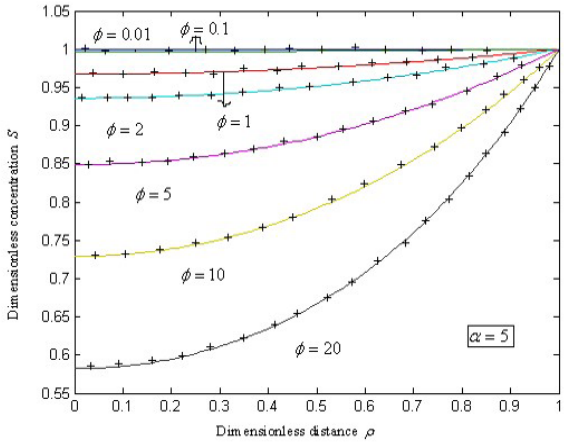

Figure 3.3: Influence of dimensionless module α on the concentration profile of substrate S obtained from our approximate solution presented in this work (equation (3.14) solid line) and from the simulation result (plus line). The plot was constructed for $\phi = 2$.

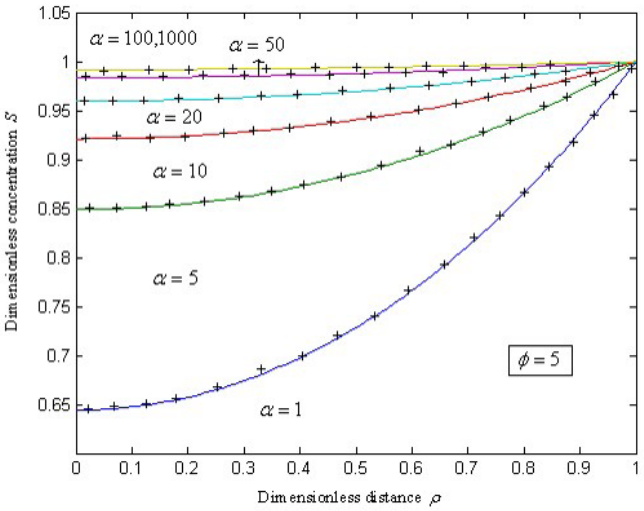

Figure 3.4: Influence of dimensionless module α on the concentration profile of substrate S obtained from our approximate solution presented in this work (equation (3.14), solid line) andfrom the simulation result (plus line). The plot was constructed for ϕ = 5.

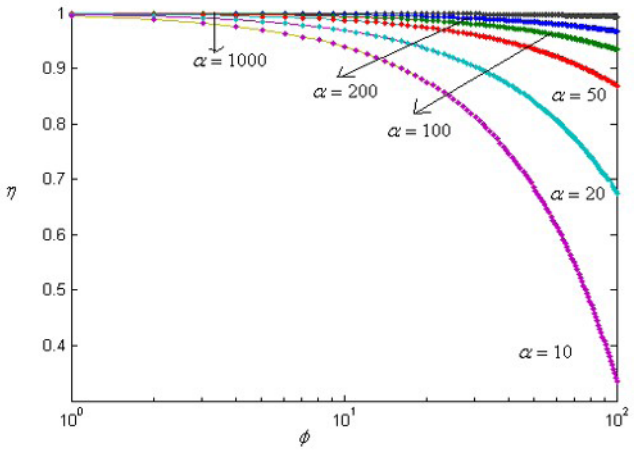

Figure 3. 5: Influence of dimensionless module α on effectiveness factor η obtained from our approximate solution presented in this work (equation (3.15), solid line) and from the simulation result (dotted line).

3.6. Conclusions

The time independent non-linear reaction/diffusion equation in immobilized enzyme system has been formulated and solved analytically. An approximate analytical expression for the concentration and effectiveness factor under steady state conditions are obtained by using the Homotopy perturbation method. The primary results of our work were simple approximate calculation of concentration and effectiveness factor for all values of parameters ϕ and α. This method can be applied to find the solution of all other non-linear reaction diffusion equations in immobilized enzymes for various complex boundary conditions.

3.7 Appendix 3.A

Basic concept of the Homotopy perturbation method (HPM)

We outline the basic idea of Homotopy perturbation method. This method has eliminated the

limitations of the traditional perturbation methods. On the other hand it can take full advantage of the traditional perturbation techniques, so there has been a considerable deal of research in applying homotopy technique for solving various strongly non-linear equations. To explain this method, let us consider the following function

$$A(u) - f(r) = 0, \quad \mathrm{r} \in \Omega \tag{3.A1}$$

with the boundary conditions of

$$B(u, \frac{\partial \mathrm{u}}{\partial n}) = 0, \ \ r \in \Gamma \tag{3.A2}$$

where A, B, $f(r)$ and Γ denote a general differential operator, a boundary operator, a known analytical function and the boundary of the domain Ω, respectively. Generally speaking, the operator A can be divided into a linear part L and a non-linear part N. equation (3.10) can therefore be written as

$$L(u) + N(u) - f(r) = 0 \tag{3.A3}$$

By the homotopy perturbation technique, we construct a homotopy $v(r, p) : \Omega \times [0,1] \to R$ which satisfies

$$H(v, p) = (1 - p)[L(v) - L(u_0)] + p[A(v) - f(r)] = 0. \qquad p \in [0,1], \ r \in \Omega \tag{3.A4}$$

or

$$H(v, p) = L(v) - L(u_0) + pL(u_0) + p[N(v) - f(r)] = 0. \tag{3.A5}$$

where $p \in [0,1]$ is an embedding parameter, and u_0 is an initial approximation of equation (3.A1) which satisfies the boundary conditions. Obviously from equations (3.A4) and (3.A5), we will have

$$H(v,0) = L(v) - L(u_0) = 0 \tag{3.A6}$$

$$H(v,1) = A(v) - f(r) = 0. \tag{3.A7}$$

when $p = 0$ equation (3.A4) or equation (3.A5) becomes a linear equation; when $p = 1$ it becomes a non-linear equation. So the changing process of p from zero to unity is just that of $L(v) - L(u_0) = 0$ to $A(v) - f(r) = 0$. We can first use the embedding parameter p as a "small parameter", and assume that the solutions of equations (3.A4) and (3.A5) can be written as a power series in p

$$v = v_0 + pv_1 + p^2 v_2 + ... \tag{3.A8}$$

Setting $p = 1$, results in the approximate solution of equation (3.A1):

$$u = \lim_{p \to 1} v = \mathrm{v}_0 + v_1 + v_2 + \ldots\ldots \quad (3.A9)$$

The combination of the perturbation method and the Homotopy method is called the Homotopy perturbation method.

3.8. Appendix 3.B

Solution of the equation (3.10) using Homotopy perturbation method.

In this appendix, we indicate how equation (3.14) in this paper is derived. To find the solution of equation (3.10), we first construct a Homotopy as follows:

$$(1-p)\left[\frac{d^2S}{d\rho^2} + \frac{2}{\rho}\frac{dS}{d\rho}\right] + p\left[\frac{d^2S}{d\rho^2} + \frac{2}{\rho}\frac{dS}{d\rho} + \frac{S}{\alpha}\frac{d^2S}{d\rho^2} + \frac{2S}{\rho\alpha}\frac{dS}{d\rho} - \frac{\phi\, S}{\alpha}\right] = 0 \quad (3.B1)$$

and the initial approximations are as follows:

$$\rho = \mathrm{O};; \quad \frac{dS}{d\rho} \quad (3.B2)$$

$$\rho = 1;\ S_0 = 1 \quad (3.B3)$$

$$\rho = 1;\ S_i = 1 \quad (3.B4)$$

$$\forall\ i = 1,\ 2, \ldots\ldots \quad (3.B5)$$

and

$$S = S_0 + pS_1 + p^2 S_2 + p^3 S_3 + \ldots\ldots \quad (3.B6)$$

Substituting equation (3.B6) into equation (3.B1) and arranging the like coefficients of powers p, we can obtain the following differential equations

$$p^0: \quad \frac{d^2S_0}{d\rho^2} + \frac{2}{\rho}\frac{dS_0}{d\rho} = 0 \quad (3.B7)$$

$$p^1: \quad \frac{d^2S_1}{d\rho^2} + \frac{2}{\rho}\frac{dS_1}{d\rho} + \frac{S_0}{\alpha}\frac{d^2S_0}{d\rho^2} + \frac{2S_0}{\rho\alpha}\frac{dS_0}{d\rho} - \frac{\phi\, S_0}{\alpha} = 0 \quad (3.B8)$$

$$p^2: \quad \frac{d^2S_2}{d\rho^2} + \frac{2}{\rho}\frac{dS_2}{d\rho} + \frac{S_1}{\alpha}\frac{d^2S_1}{d\rho^2} + \frac{2S_1}{\rho\alpha}\frac{dS_1}{d\rho} - \frac{\phi\, S_1}{\alpha} = 0 \quad (3.B9)$$

Solving equation (3.B7) to (3.B9) using reduction of order (see Appendix 3.C) for solving the equation (3B8), and using the boundary conditions (3.B4) to (3.B5), we can find the following results

$$S_0(\rho) = 1 \quad (3.B10)$$

$$S_1(\rho) = \frac{\phi}{6\alpha}(\rho^2 - 1) \quad (3.B11)$$

$$S_2(\rho)=\frac{\phi^2}{120\alpha^2}\left(\rho^4-1\right)+\frac{\phi^2}{36\alpha^2}\left(1-\rho^2\right)+\frac{\phi^2}{120\alpha^3}\left(1-\rho^4\right)-\frac{\phi^2}{36\alpha^3}\left(1-\rho^2\right) \tag{3.B12}$$

According to the HPM, we can conclude that

$$S(\rho)=\lim_{p\to 1} S(\rho)=S_0+S_1+S_2..... \tag{3.B13}$$

After putting equations (3.B10), (3.B11) and (3.B12) into equqtion (3.B13). The final results can be described in equation (3.5) in the text. The remaining components of $u_n(x)$ and $v_n(x)$ be completely determined such that each term is determined by the previous term.

3.8. Appendix 3.C

In this appendix, we derive the solution of equation (3.B8) by using the reduction of order. The equation (3.B8) can be written in the form:

$$\frac{\mathrm{d}^2\overline{u_1}}{\mathrm{d}\rho^2}+P\frac{\mathrm{d}\overline{u_1}}{\mathrm{d}\rho}+Q\overline{u_1}=R \tag{3.C1}$$

where

$$P=\frac{2}{\rho};\ Q=0 \text{ and } R=\frac{\phi}{\alpha} \tag{3.C2}$$

Let the solution of equation (3.C1) be

$$u_1=c(\rho)v(\rho) \tag{3.C3}$$

Substituting equation (3.C3) in (3.C1), we get

$$\frac{\mathrm{d}^2v}{\mathrm{d}\rho^2}+P_1\frac{\mathrm{d}v}{\mathrm{d}\rho}+Q_1v=R_1 \tag{3.C4}$$

where

$$P_1=P+\frac{2}{c}\frac{d}{d\rho},\ Q_1=\frac{1}{c}\left(\frac{d^2c}{d\rho^2}+P\frac{dc}{d\rho}+Qc\right) \text{ and } R_1=\frac{R}{c} \tag{3.C5}$$

Now to remove the first derivative, we can choose the coefficient of the first derivative in equation (3.C4) is zero ($P_1=0$). We have

$$\frac{2}{c}\frac{\mathrm{d}c}{\mathrm{d}\rho}+P=0 \tag{3.C6}$$

Solving equation (3.C6), we can obtain *c* as follows:

$$c=e^{-1/2\int PdP}=\frac{1}{\rho} \tag{3.C7}$$

Now the given equation (3.C4) reduces to

$$v''+Q_1v=R_1 \tag{3.C8}$$

Substituting the value of Q_1 and U_2 in equation (3.C8) we obtain,

$$v'' = \frac{\phi x}{\alpha} \tag{3.C9}$$

Solving the above equation (3.C9), we get

$$v = A\rho + B + \frac{\phi \rho^3}{6\alpha} \tag{3.C10}$$

Substituting (3.C7) and (3.C10) in (3.C3), we have

$$u_1 = A + \frac{B}{\rho} + \frac{\phi \rho^2}{6\alpha} \tag{3.C11}$$

Using the boundary conditions (equations (3.B4) and (3.B5)), we can obtain the value of the constants *A* and *B*. Substituting the value of the constants *A* and *B* in the equation (3.C11) we obtain the equation (3.B11). Similarly we can solve the other differential equation. (3.B9), using the reduction of order method.

3.9. Appendix 3.D

NOMENCLATURE

Symbol	Meaning	Usual dimension
C_P	Product concentration inside the spherical particle	Mole/cm^3
C_{PE}	Equilibrium product concentration	Mole/cm^3
C_{PR}	local product concentration at particle surface	Mole/cm^3
C_S	Substrate concentration inside the spherical particle	Mole/cm^3
C_{SE}	Equilibrium substrate concentration	Mole/cm^3
C_{SR}	local substrate concentration at particle surface	Mole/cm^3
D_P	Effective product diffusivity inside the particle	Cm^2 sec^{-1}
D_S	Effective substrate diffusivity inside the particle	Cm^2 sec^{-1}
K_{eq}	equilibrium constant	None
K_M	Michaelis constant	Mole/cm^3
K_P	Competitive product inhibition constant	None
r	radial coordinate of the particle	Cm
R	radius of the particle	Cm
S	dimensionless substrate concentration, defined as C_S/C_{SR} for the two-parameters model	Mole/cm^3
V_m	maximum reaction rate per unit of catalytic particle volume	Mole/cm^3 sec

V_S	local reaction rate per unit of catalytic particle volume	Mole/cm^3 sec
Greek symbols		
α	dimensionless module for two parameter model	None
ϕ	dimensionless module for two parameter model	None
η	effectiveness factor	None
ρ	dimensionless particle radial coordinate	None

3.10. References

1. J. E. Bailey and D. F. Ollis, Biochemical Engineering Fundamentals (2nd ed.)., McGraw-Hill, New York, 1986.

2. J. M. Engasser and C. Horvath, Effect of internal diffusion in heterogeneous enzymatic systems: evaluation of true kinetic parameters and substrate diffusivity, J. Theor. Biol, 42 137-155, 1973.

3. A. Tuncel, A diffusion-reaction model for -chymotrypsin carrying uniform thermosensitive gel beads, J. Appl. Polym. Sci. 74 , 1025-1034, 1999.

4. A. L. Paiva and F. X . Malcata. Reversible reaction and diffusion within a porous catalyst slab, Chem. Eng. Sci., 52 (23), 4429-4432, 1997.

5. G. Xiu, L. Jiang and P. Li, Mass-transfer limitations for immobilized enzyme-catalyzed kinetic resolution of racemate in a batch reactor, Ind. Eng Chem. Res. 39, 4054-4062, 2000.

6. J. M. Engasser and P. Hisland, Diffusional effects on the heterogeneous kinetics of two- substrate enzymic reactions, J. Theor. Biol. 77, 427-440, 1979.

7. P. R. Rony, Multiphase catalysis. II. Hollow fiber catalysts, Biotechnol. Bioeng. 13, 431- 447, 1971.

8. M. Moo-Young and T. Kobayashi, Effectiveness factors for immobilized enzyme reactions, J. Can. Chem. Eng. 50, 162-167, 1972.

9. T. Kobayashi and K. J. Laidler. Effectiveness factor calculations for immobilized enzyme catalysts, Biochim. et Biophys. Acta. 1, 302-311, 1973.

10. D. J. Fink, T. Y. Na and J. S. Suchltz. Effectiveness factor calculations for immobilized enzyme catalysts, Biotechnol. Bioeng. 15, 879-888, 1973.

11. J. M. Engasser and J. C. Horvath, Metabolism: Interplay of Membrane Transport and Consecutive Enzymic Reaction, Theor. Biol. 42, 137-155, 1973.

12. D. R. Marsh, Y. Y. Lee and G.T. Tsao, Immobilized glucoamylase on porous glass, Biotechnol. Bioeng. 15, 483-492, 1973.

13. B. K. Hamilton, C. R. Cardner and C. K. Colton. Effect of Diffusional Limitations on. Lineweaver-Burk Plots for Immobilized Enzymes, AICHE J. 20, 503-510, 1974.

14. B. J. Rovito and J. R. Kittrell, Film and pore diffusion studies with immobilized glucose Oxidase, Biotechnol. Bioeng. 15, 143-161, 1973.

15. J. M. Engasser. The experimental results accorded quantitatively with the theory of diffusion limitation, Biochim. Biophys. Acta. 526, 301-310, 1978.

16. A. Marc and J. M. Engasser, Influence of substrate and product diffusion on the heterogeneous kinetics of enzymic reversible reactions, J. Theor. Biol. 94, 179-189, 1982.

17. R. Goldman, O. Keden, I. H. Silman S. R. Caplan and E. Katchalski, Papain-collodion membranes. I. Preparation

and properties, Biochemistry. 7, 486-500, 1968.

18. J. M. Engasser and C. Horvath, Inhibition of Bound Enzymes. II. Characterization of Product Inhibition and Accumulation, Biochemistry. 13, 3849-3854, 1974.

19. P. A. Ramachandran, Solution of immobilized enzyme problems by collocation methods, Biotechnol. Bioeng, 17, 211-226, 1975.

20. A. Manjon, J. L. Iborra, J. L. Gomez, E. Gomez, J. Bastida and A. Bodalo, Evaluation of

The effectiveness factor along immobilized enzyme fixed-bed reactors: design for a reactor with naringinase covalently immobilized into glycophase-coated porous glass, Biotechnol. Bioeng. 30, 491-497, 1987.

21. A. Bodalo Santoyo, J. L. G´omez Carrasco, E. G´omez G´omez, J. Bastida Rodr´ıguez

and E. Mart´ınez Morales, Transient stirred tank reactors operating with immobilized enzyme systems: analysis and simulation models and their experimental checking, Biotechnol. Progr. 9, 166–173, 1993.

22. A. Bodalo, J. L. G´omez, E. G´omez, J. Bastida and M. F. M´aximo, Fluidized bed reactors operating with immobilized enzyme systems: design model and its experimental verification, Enzyme Microb. Technol. 17, 915–922, 1995.

23. A. E. AL-Muftah and I. M. Abu-Reesh, Effects of internal mass transfer and product inhibition on a simulated immobilized enzyme-catalyzed reactor for lactose hydrolysis, Biochem. Eng. J. 23, 139–153, 2005.

24. A.E. AL-Muftah and I.M. Abu-Reesh, Effects of simultaneous internal and external mass transfer and product inhibition on immobilized enzymecatalyzed reactor, Biochem. Eng. J. 27, 167–178, 2005.

25. S.D. Keegan, N.J. Mariani, S.P. Bressa, G.D. Mazza and G.F. Barreto, Approximation of the effectiveness factor in catalytic pellets, Chem. Eng. J. 94, 107–112, 2003.

26. M. Szukiewicz and R. Petrus, Approximate model for diffusion and reaction in a porous pellet and an effectiveness factor, Chem. Eng. Sci. 59, 479–483, 2004.

27. X. Li, X.D. Chen and N. Chen, A third-order approximate solution of the reaction- diffusion process in an immobilized biocatalyst particle, Biochem. Eng. J. 17, 65–69, 2004.

28. B. Carnahan, H.A. Luther and J.O. Wilkes, Applied Numerical Methods, Wiley, New York, 1969.

29. J. Villadsen and M. L. Michelsen, Solution of Differential Equation Models by Polynomial Approximation., New York: Prentice-Hall, Englewood Cliffs, 1978.

30. X. B. Chen., Y. Sui., H. P. Lee., H. X. Bai., P. Yu., S. H. Winoto and H. T. Low. Mass transport in a microchannel bioreactor with a porous wall,ASME J. Biomech. Engrg., 132(6), 061001, 2010.

31. X. B. Chen., Y. Sui., Y. P. Cheng., H. P. Lee., P. Yu., S. H. Winoto and H. T. Low, Mass transport in a microchannel enzyme reactor with a porous wall: Hydrodynamic modeling and applications, Biochem. Eng. J., 52, 227-235, 2010.

32. A. Bodalo.,J. L. Gomez., E. Gomez., J. Bastida., J. L. Iborra and A. Manjon, Analysis of diffusion effects on immobilized enzyme on porous supports with reversible Michaelis-Menten kinetics, Enzyme Microb. Technol., 8, 433-438, 1986.

33. A. Bodalo, J.L.Gomez,E. Gomez.,J. Bastida, J.L Iborra, and A. Manjon, Analysis of diffusion effects on immobilized enzyme on porous supports with reversible Michaelis- Menten kinetics, Enzyme Microb. Technol. 8, 433-438, 1986.

34. J. H. He, An elementary introduction to recently developed asymptotic methods and nanomechanics in textile engineering, Int. J. Modern. Physics., 22, 3487-3578, 2008.

35. J. H. He, Approximate analytical solution for seepage flow with fractional derivatives in porous media, Comput.

Methods. Appl. Mech. Engrg, 167, 57, 1998.

36. J. H. He, Application of homotopy perturbation method to nonlinear wave equations, Appl. Math. Comput., 26, 695, 2005.

37. J. H. He, Homotopy perturbation method for solving boundary value problems, Phys. Lett. A., 350, 87, 2006.

38. A. Eswari, and L. Rajendran, Analytical solution of steady state current at a micro disk biosensor, J. Electroanal. Chem., 641, 35-44, 2010.

39. A. Meena, and L. Rajendran, Mathematical modeling of amperometric and biosensors and system of non-linear equations-Homotopy perturbation approach, J. Electroanal. Chem., 644, 50-59, 2010.

40. A. Meena and L. Rajendran, Analytical solution of system of coupled non-linear reaction diffusion equations. Part I: Mediated electron transfer at conducting polymer ultra microelectrodes, J. Electroanal. Chem., 647, 103-116, 2010.

Non-linear boundary value problems in immobilized glucoamylase kinetics

Chapter 4

4. Solution of non-linear boundary value problems in immobilized glucoamylase kinetics

4.1. Introduction

Flow reaction calorimetry has several advantages over a batch calorimetry method. The operation at a calorimetric experiment can be made exceedingly simple and equilibration time prior to the experiment can be omitted. Mixing of reactants can be achieved without the presence of a gaseous phase which is of great importance when experiments are performed with volatile liquids and in micro-calorimetric expriments where very small condensation-evaporation effects may affect the result. Surface adsorption effects which may cause seious systematic errors in micro calorimetry can be neglected if a steady liquid flow is allowed to continue until possible wall reactions have occurred [1]. Immobilized biocatalysts (IMB)-enzymes or whole cells- are used in various areas of analytical, medical, and industrial applications. Basically, enzyme kinetic parameters cannot be determined experimental data. For this purpose many experimental techniques can be used, that are more or less laborious and time consuming. Reaction kinetics of carboxyl esterase's depends strongly on the nature of substrate. The hydrolysis of different substrate activation [2] or it can follow the simple Michaelis-Menten kinetics [3].

Stefuca et al. [4] have described the principles and applications of flow calorimetry (FC) in the investigation of the IMB properties. One of the last improvements of this technique was the introduction of an "auto calibration" principle based on reaction solution recirculation enabling to determine true reaction rate of biocatalyst reaction without any requirement of an additional analytical technique [5]. Vladimir Stefuca et al. [6] have derived the experimental data were treated by mathematical modelling based on material and heat balances of the reaction system. Recently, Fedor Malik [7] has developed the mathematical model describing the enzyme reaction, mass transfer and heat effects in the calorimetric system.

To my knowledge no rigorous analytical solutions of the substrate of phenyl acetate hydrolysis with steady-state conditions for all values of parameters α, β and γ_E have been reported. The purpose of this chapter is to derive approximate analytical expressions for the steady-state concentration of substrate using Adomian decomposition method, Homotopy analysis and perturbation method.

4.2. Mathematical formulation of the problem

The experimental set- up used for the capacity is depicted in **(figure.4.1)**. The main part

of the system thermostatic cell through immobilized enzyme column. The column was operated packed bed reactor. The temperature difference between the column input and output ΔT , is measured by thermistors and registered by a personal computer. The system was kept at temperature of 303.15K, while the buffer solution was continuously pumped through the column with constant flow rate of 1ml/min.

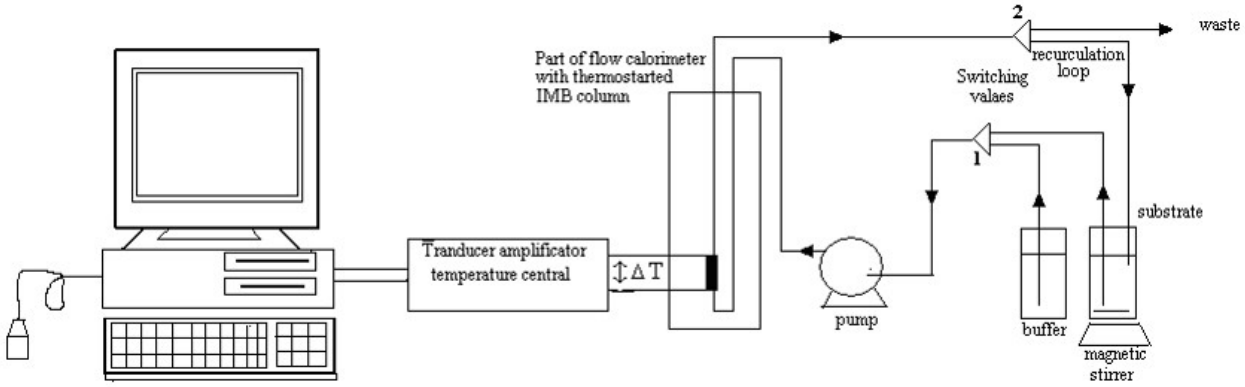

Figure 4.1: Experimental set-up of flow calorimetry.

The experiment was started by replacing the buffer solution by the substrate solution containing 1-200 g/l of MDX in 0.1 M acetate buffer (pH 4.7). Two techniques of measurement were applied: single flow mode and total recirculation mode. The single flow mode was performed with the switching valve 2 opened to the waste [7]. The substrate concentration gradient on the particle surface was calculated by the equation of substrate balance in the particle [7]:

$$\frac{\partial c_{SP}}{\partial t} = D_e\left(\frac{\partial^2 c_{SP}}{\partial r^2} + \frac{2}{r}\frac{\partial c_{SP}}{\partial r}\right) - \frac{V_m c_{SP}}{K_m + c_{SP} + (c_{SP}^{\,2} / K_i)} \tag{4.1}$$

The equation must be solved subject to the following initial and boundary conditions:

$$c_{SP} = 0 \quad \text{at} \quad t = 0,\ 0 \le r \le 1, \tag{4.2}$$

$$\frac{dc_{SP}}{dr} = 0 \ \text{at}\ r = 0, \tag{4.3}$$

$$c_{SP} = c_S \ \text{at}\ r = R_p, \tag{4.4}$$

Where c_{SP} is the substrate concentration in the particle, c_S is the phenyl acetate concentration, D_e is the diffusion coefficient, V_m, K_m, K_i are the kinetic parameters and r is the particle radial co-ordinate, A_n is the particle radius. We can write the steady state equation as [7]:

$$D_e\left(\frac{d^2 c_{SP}}{dr^2} + \frac{2}{r}\frac{dc_{SP}}{dr}\right) - \frac{V_m c_{SP}}{K_m + c_{SP} + (c_{SP}^{\,2} / K_i)} = 0 \tag{4.5}$$

The system governs the substrate concentration c_{SP} when there is no competitive inhibition in the reaction. The non-linear ODE (equation (4.5)) is made dimensionless by defining the following parameters:

$$x = \frac{r}{R_p};\ U = \frac{c_{SP}}{c_S};\quad \gamma_E = \frac{R_p^2 V_m}{D_e K_m},\ \alpha = \frac{c_S}{K_m},\ \beta = \frac{{c_S}^2}{K_i K_m} \tag{4.6}$$

Where γ_E denote the reaction diffusion parameter, x is the dimensionless distance and $U(x)$ is the dimensionless concentration. Here α and β denotes the saturation parameters. The above equation (4.5) reduces to the following dimensionless form

$$\frac{d^2U}{dx^2} + \frac{2}{\rho}\frac{dU}{dx} - \frac{\gamma_E U}{1+\alpha U+\beta U^2} = 0 \tag{4.7}$$

The corresponding boundary conditions are

$$U = 1 \ \ at\ x = 1 \tag{4.8}$$

$$\frac{dU}{dx} = 0 \ \text{ at } x = 0 \tag{4.9}$$

4.3. Solution of boundary value problem using Adomian decomposition method

Adomian's decomposition method has been successfully applied to linear and nonlinear problems.One of its advantages is that it provides a rapid convergent solution series [8].

However, the method applied to nonlinear equations does not seem to be fast enough to be a efficient method to solve these kind of equations and one can find in the open literature some modifications proposed by several authors [9-13]. By applying the Adomian's decomposition method, a new iterative method to compute nonlinear equations is developed and is presented in this work. The Adomian decomposition method is an extremely simple method [9-13] to solve the non-linear differential equations. First iteration is enough. Furthermore, the obtained result is of high accuracy. Using this Adomian decomposition method (see appendix 4.A and 4.B), the solution of equation (4.7) becomes:

$$U(x) = 1 - \frac{\gamma_E}{6(1+\alpha+\beta)} + \frac{7\gamma_E^2(1-\beta)}{360(1+\alpha+\beta)^3} + \left(\frac{\gamma_E}{6(1+\alpha+\beta)} - \frac{\gamma_E^2(1-\beta)}{36(1+\alpha+\beta)^3}\right)\left(\frac{x^2}{6}\right) + \frac{\gamma_E^2(1-\beta)}{6(1+\alpha+\beta)^3}\left(\frac{x^4}{20}\right) \tag{4.10}$$

4.4. Solution of boundary value problem using Homotopy analysis method

Perturbation methods are the most famous analytic techniques for nonlinear problems, which are widely applied in science and engineering. In 1992, the Homotopy, a traditional concept in topology, was used by Liao [14] to propose an approximation technique for nonlinear problems, namely the homotopy analysis method (HAM). Using the concept of the Homotopy, a nonlinear problem is transformed into a sequence of linear sub-problems that are easy to solve by means of the symbolic computation software. In 1997 Liao [14] further generalized

the HAM by introducing an auxiliary nonzero parameter (called today the convergence-control parameter). Different from perturbation techniques, the HAM does not depend upon any small physical parameters, and besides provides great freedom to choose different base functions to approximate nonlinear problems. Especially, different from all other analytic approximation methods, the so-called convergence-control parameter of the HAM provides us a convenient way to ensure the convergence of series solution. Thus, the HAM overcomes the restrictions of the perturbation methods and therefore is more general. With these advantages and having the aid of high-performance computer and symbolic computation software, the HAM has been widely applied to solve many types of nonlinear differential equations in science, engineering and finance [15]. Using this HAM (see appendix 2.A and 4.C) we obtain, the concentration of substate as follows:

$$U(x)=1+\frac{h\gamma_E}{6}\left(h+2+h(1+\alpha+\beta)+\frac{7h\gamma_E}{60}\right)-\left(\frac{h\gamma_E}{6}(h+2+h(1+\alpha+\beta))+\frac{h^2\gamma_E^2}{36}\right)x^2+\frac{h^2\gamma_E^2x^4}{120} \tag{4.11}$$

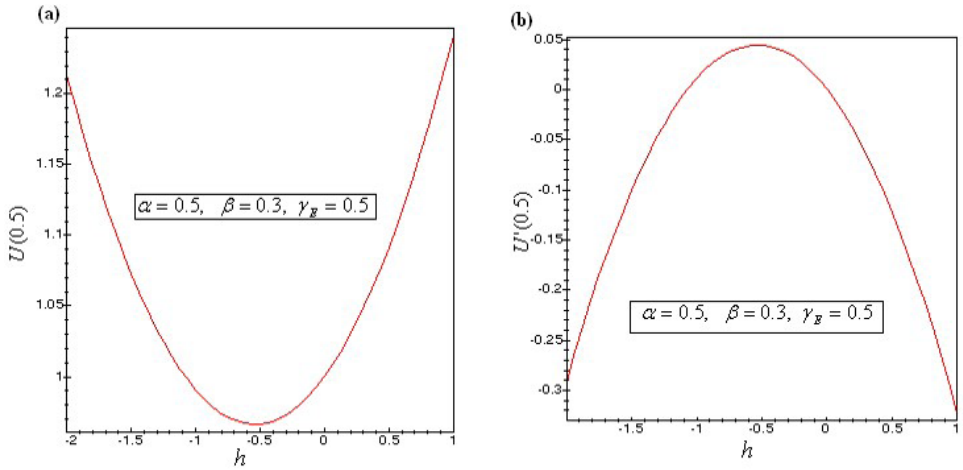

Figure.4.9: The *h* curves indicate the convergence region, for $\alpha = 0.5$, $\beta = 0.3$ and $\gamma_E = 0.5$

4.5. Solution of boundary value problem using Homotopy perturbation method

The Homotopy perturbation method which doesn't need small parameter is implemented for solving the differential equations and it is predicted that HPM can be founded widely applicable in engineering and in cases that don't have exact solution this method can be used as semi-exact solution. Homotopy perturbation method yields a very rapid convergence and usually, one iteration leads to high accuracy of solution [17-25]. The Homotopy perturbation method is a high accuracy method. Using this method (see appendix 3.A and 4.D) we obtain

$$U(x)=1+\frac{\gamma_E}{6}\left(\frac{7\gamma_E}{6}-1+\alpha+\beta\right)-\left(\frac{\gamma_E}{6}-1+\alpha+\beta\right)\frac{\gamma_E x^2}{6}+\frac{\gamma_E^2 x^4}{120} \tag{4.12}$$

4.6. Numerical simulation

The non-linear differentials equations (4.7 - 4.9) are also solved by numerical methods. The function bvp4c in Matlab software which is a function of solving two-point boundary value problems (BVPs) for ordinary differential equations is used to solve this equation. The

Matlab program is also given in appendix G. Its numerical solution is compared with Adomian decomposition method, Homotopy analysis and perturbation method in Table 4.2-4.5 and it gives satisfactory result when α≤1 and β≤1.

4.7. Results and discussion

The primary result of this work is the first approximate and simple expression of concentrations of substrate (equations (4.10) (ADM), (4.11) (HAM) and (4.12) (HPM)). figures. 4..2-4.5 show the analytical expression of concentration of substrate $U(x)$ for various values of dimensionless reaction diffusion parameter γ_E and saturation parameters α, β. From these figures.4.2-4.5, it is inferred that the value of the concentration of substrate $U(x)$ increases when dimensionless reaction diffusion parameter γ_E decreases. Also in these figures 4.2 to 4.5, it is known that the value of the concentration of substrate increases gradually and attains the maximum at the boundary $x = 1$).

The normalized numerical simulation of three dimensional substrate concentrations $u(x)$ is shown in figures. 4.6-4.8**.** The time independent concentration $g(x)$ is represented in figures 4.6-4.8 for fixed value of $\beta = 0.001$. Concentration $N(y)$ is slowly decreasing when γ_E is increasing. Then the concentration of $u(x) = 1$ when $x = 1$ and also for all values of γ_E, α and β. In these figure, it should be noted that the value of the concentration of substrate decreases for all values of γ_E. From this Figures, it is apparent that the value of the concentration of substrate increases for various values of α increases.

Table 4.1: Numerical values of the parameters used in this work. The fixed values of the dimension parameters are

$c_s = 3.24,\ 5.932$ mmoldm^{-3} $D_e = 9.4 \times 10^{-9}$ $K_i = 25, 17 mmoldm^3$ $K_m = 9,6.4$ mmoldm^3

, , $V_m = 13.7, 11.1$ mK and $R_p = 0.001$. These are dimensional parameters used in Fedor Malik et al. [7].Q

Parameter	Unit	Numerical value of parameter used in Fedor-Malik et al. [7]	Numerical value of parameter used in this work			
			Fig. 4. 2	Fig. 4. 3	Fig. 4. 4	Fig. 4. 5
$\alpha = \frac{c_S}{K_m}$	---	0.3 to 1.07	0.1	0.01	0.2	0.05
$\beta = \frac{c_S^2}{K_i K_m}$	---	0.07 to 0.3	0.01	0.1	0.5	0.0001
x	---	0 to 1	0 to 1	0 to 1	0 to 1	0 to 1
$\gamma_E = \frac{R_p^2 V_m}{D_e K_m}$	---	0 to 173.437	0.1, 0.5, 1	0.02, 0.5, 1, 2.5	0.1, 0.5, 2	0.01, 0.1, 0.6,1, 3

Table 4.2: Comparison of dimensionless substrate concentration $U(x)$ with numerical solution for various small values of when $\alpha = 0.1, \beta = 0.001$.

	Dimensionless substrate concentration $U(x)$ when $\alpha = 0.1,\ \beta = 0.001$																			
x	$\gamma_E = 0.1$							$\gamma_E = 0.5$							$\gamma_E = 1$						
	Simulation	ADM Eq. (4.10)	Error %	HA Eq. (4.11)	Error %	HPM Eq. (4.12)	Error %	Simulation	ADM Eq. (4.10)	Error %	HAM Eq. (4.11)	Error %	HPM Eq. (4.12)	Error %	Simulation	ADM Eq. (4.10)	Error %	HAM Eq. (4.11)	Error %	HPM Eq. 4.(12)	Error %
0	0.9837	0.9837	0	0.9879	0.43	0.9837	0	0.9220	0.9223	0.03	0.9405	2.01	0.9224	0.04	0.8522	0.8539	0.20	0.8833	0.28	0.8546	3.65
0.2	0.9844	0.9844	0	0.9884	0.41	0.9844	0	0.9251	0.9254	0.03	0.9429	1.92	0.9255	0.04	0.8580	0.8554	0.19	0.8880	0.26	0.8602	3.50
0.4	0.9864	0.9864	0	0.9899	0.36	0.9864	0	0.9345	0.9347	0.02	0.9502	1.68	0.9348	0.03	0.8754	0.8767	0.15	0.9021	0.21	0.8772	3.05
0.6	0.9897	0.9897	0	0.9924	0.27	0.9897	0	0.9502	0.9504	0.02	0.9623	1.27	0.9504	0.02	0.9049	0.9057	0.09	0.9257	0.13	0.9061	2.30
0.8	0.9943	0.9943	0	0.9958	0.16	0.9943	0	0.9725	0.9726	0.01	0.9793	0.70	0.9726	0.01	0.9471	0.9475	0.04	0.9591	0.06	0.9477	1.27
1	1.0000	1.0000	0	1.0000	0	1.0000	0	1.0000	1.0000	0	1.0000	0	1.0000	0	1.0000	1.0000	0	1.0000	0	1.0000	0
Average % of deviation			0		0.27		0		0.02			1.26		0.03		0.11			0.16		1.27

Table 4.3(a): Comparison of dimensionless substrate concentration $U(x)$ with numerical solution for various small values of γ_E when $\alpha = 0.01, \beta = 0.1$

x	Dimensionless substrate concentration $U(x)$ when $\alpha = 0.01, \beta = 0.1$													
	$\gamma_E = 0.02$							$\gamma_E = 0.5$						
	simulation	ADM	Error %	HAM	Error %	HPM	Error %	simulation	ADM	Error %	HAM	Error %	HPM	Error %
0	0.9970	0.9970	0	0.9977	0.07	0.9970	0	0.9281	0.9281	0	0.9424	1.54	0.9307	0.28
0.2	0.9971	0.9971	0	0.9977	0.06	0.9972	0.01	0.9309	0.9309	0	0.9447	1.48	0.9334	0.27
0.4	0.9975	0.9975	0	0.9980	0.05	0.9975	0	0.9394	0.9394	0	0.9516	1.30	0.9715	0.23
0.6	0.9981	0.9981	0	0.9985	0.04	0.9981	0	0.9537	0.9537	0.03	0.9630	0.98	0.9552	0.16
0.8	0.9989	0.9989	0	0.9992	0.03	0.9989	0	0.9738	0.9738	0	0.9792	0.56	0.9746	0.08
1	1.0000	1.0000	0	1.0000	0	1.0000	0	1.0000	1.0000	0	1.0000	0	1.0000	0
Average % of deviation		0		0.04		0.002		0.01			0.98		0.17	

Table 4.3(b): Comparison of dimensionless substrate concentration $U(x)$ with numerical solution for various small values of γ_E when $\alpha = 0.01, \beta = 0.1$.

x	Dimensionless substrate concentration $U(x)$ when $\alpha = 0.01, \beta = 0.1$													
	$\gamma_E = 1$							$\gamma_E = 0.5$						
	simulation	ADM	Error %	HAM	Error %	HPM	Error %	simulation	ADM	Error %	HAM	Error %	HPM	Error %
0	0.8621	0.8626	0.06	0.8871	2.90	0.8711	1.04	0.6955	0.7046	1.31	0.7346	5.62	0.7507	7.09
0.2	0.8674	0.8679	0.58	0.8915	2.78	0.8759	0.98	0.7065	0.7151	1.23	0.7447	5.41	0.7587	7.39
0.4	0.8835	0.8839	0.05	0.9049	2.42	0.8906	0.81	0.7402	0.7473	0.96	0.7754	4.76	0.7836	5.86
0.6	0.9105	0.9108	0.04	0.9273	1.85	0.9156	0.56	0.7982	0.803	0.60	0.8274	3.66	0.8284	3.78
0.8	0.9491	0.9493	0.02	0.9589	1.03	0.9517	0.28	0.8834	0.8858	0.27	0.9017	2.07	0.8983	1.68
1	1.0000	1.0000	0	1.0000	0	1.0000	0	0.9995	1.0000	0.05	1.0000	0.05	1.0000	0.05
Average % of deviation		0.04		1.83		0.61		0.74			3.59		4.45	

Table 4.4: Comparison of dimensionless substrate concentration $U(x)$ with numerical solution for various small values of γ_E when $\alpha = 0.2, \beta = 0.5$.

Dimensionless substrate concentration $U(x)$ when $\alpha = 0.2, \beta = 0.5$																			
x	$\gamma_E = 0.1$							$\gamma_E = 0.5$							$\gamma_E = 2$						
	Simulation	ADM Eq. (4.7)	Error %	HAM Eq. (4.8))	Error %	HPM Eq. (4.9)	Error %	Simulation	ADM Eq. (4.7)	Error %	HAM Eq. (4.8)	Error %	HPM Eq. (4.9)	Error %	Simulation	ADM Eq. (4.7)	Error %	HAM Eq. (4.8)	Error %	HPM Eq. (4.9)	Error %
0	0.9902	0.9902	0	0.9906	0.04	0.9952	0.51	0.9515	0.9515	0	0.9538	0.24	0.9799	2.99	0.9042	0.9039	0.03	0.9098	0.62	0.9694	7.22
0.2	0.9906	0.9906	0	0.9909	0.03	0.9954	0.49	0.9534	0.9534	0	0.9556	0.23	0.9806	2.86	0.9080	0.9077	0.03	0.9133	0.59	0.9703	6.86
0.4	0.9918	0.9918	0	0.9921	0.03	0.9960	0.43	0.9592	0.9592	0	0.9611	0.20	0.9828	2.46	0.9194	0.9192	0.02	0.9239	0.49	0.9732	5.85
0.6	0.9937	0.9937	0	0.9940	0.03	0.9969	0.32	0.9689	0.9689	0	0.9703	0.15	0.9866	1.83	0.9385	0.9383	0.02	0.9418	0.36	0.9785	4.26
0.8	0.9965	0.9965	0	0.9966	0.01	0.9983	0.18	0.9825	0.9825	0	0.9832	0.07	0.9923	1.00	0.9653	0.9652	0.01	0.9652	0.01	0.9871	2.26
1	1.0000	1.0000	0	1.0000	0	1.0000	0	1.0000	1.0000	0	1.0000	0	1.0000	0	1.0000	1.0000	0	1.0000	0	1.0000	0
Average % of deviation		0		0.03		0.32		0			0.15		1.85		0.02			0.34		4.41	

Table 4.5(a): Comparison of dimensionless substrate concentration $U(x)$ with numerical solution for various small values of γ_E when $\alpha = 0.5, \beta = 0.0001$.

x	Dimensionless substrate concentration $U(x)$ when $\alpha = 0.5, \beta = 0.0001$.													
	$\gamma_E = 0.01$							$\gamma_E = 0.1$						
	Simulation	ADM	Error %	HAM	Error %	HPM	Error %	Simulation	ADM	Error %	HAM	Error %	HPM	Error %
0	0.9984	0.9984	0	0.9988	0.04	0.9984	0	0.9843	0.9843	0	0.9881	0.38	0.9844	0.01
0.2	0.9985	0.9985	0	0.9989	0.04	0.9985	0	0.9849	0.9849	0	0.9886	0.37	0.9850	0.01
0.4	0.9987	0.9987	0	0.9990	0.03	0.9987	0	0.9868	0.9868	0	0.9900	0.32	0.9869	0.01
0.6	0.9990	0.9990	0	0.9992	0.02	0.9990	0	0.9899	0.9899	0	0.9924	0.25	0.9900	0.01
0.8	0.9994	0.9994	0	0.9996	0.02	0.9994	0	0.9943	0.9943	0	0.9957	0.14	0.9944	0.01
1	1.0000	1.0000	0	1.0000	0	1.0000	0	1.0000	1.0000	0	1.0000	0	1.0000	0
Average % of Deviation		0		0.03		0		0			0.25		0.01	

Table 4.5(b): Comparison of dimensionless substrate concentration $U(x)$ with numerical solution for various small values of γ_E when α = 0.5, β = 0.0001. .

Dimensionless substrate concentration $U(x)$ when $\alpha = 0.5, \beta = 0.0001$.																				
x	$\gamma_E = 0.6$							$\gamma_E = 1$							$\gamma_E = 3$					
	Simulation	ADM Eq. (4.7)	Error %	HAM Eq. (4.8)	Error %	HPM Eq. (4.9)	Error %	Simulation	ADM Eq. (4.7)	Error %	HAM Eq. (4.8)	Error %	HPM Eq. (4.9)	Error %	Simulation	ADM Eq. (4.7)	Error %	HAM Eq . (4.8)	Error %	HPM Eq. (4.9)	Error %
0	0.9105	0.9108	0.03	0.9298	2.12	0.912	0.17	0.8567	0.8581	0.16	0.8848	3.28	0.8611	0.51	0.6423	0.6750	5.09	0.6813	6.07	0.7000	8.98
0.2	0.9140	0.9143	0.03	0.9326	2.04	0.9154	0.15	0.8622	0.8635	0.15	0.8893	3.14	0.8664	0.49	0.6548	0.6855	4.69	0.6934	5.90	0.7092	8.31
0.4	0.9245	0.9247	0.02	0.9409	1.77	0.9257	0.13	0.8788	0.8798	0.11	0.9030	2.75	0.8822	0.39	0.6932	0.7183	3.62	0.7300	5.31	0.7380	6.46
0.6	0.9422	0.9423	0.01	0.9549	1.35	0.9430	0.09	0.9068	0.9075	0.08	0.9258	2.09	0.9092	0.27	0.7601	0.7771	2.24	0.7920	4.20	0.7908	4.04
0.8	0.9672	0.9673	0.01	0.9746	0.77	0.9676	0.04	0.9469	0.9472	0.03	0.9581	1.18	0.9481	0.13	0.8601	0.8681	0.93	0.8813	2.47	0.8747	1.70
1	1.0000	1.0000	0	1.0000	0	1.0000	0	1.0000	1.0000	0	1.0000	0	1.0000	0	0.9999	1.0000	0.01	1.0000	0.01	1.0000	0.01
Average % of deviation		0.02		1.34		0.07		0.09			2.08		0.30		2.76			3.99		4.92	

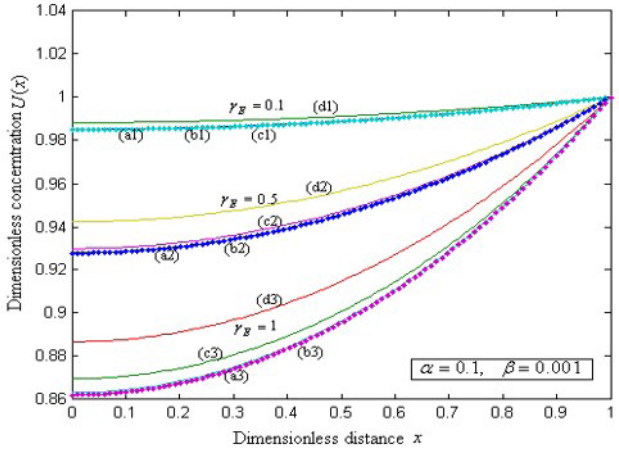

Figure 4.3: Dimensionless concentration $U(x)$ versus dimensionless distance x when α = 0.1, β = 0.001. . The curves a1, a2, a3 (ADM), b1, b2, b3 (simulation), c1, c2, c3 (HPM), d1, d2, d3 (HAM) are plotted when γ_E = 0.1, 0. 5, 1. Symbols (---) equations. (4.10)-(4.12) and (…) numerical simulation.

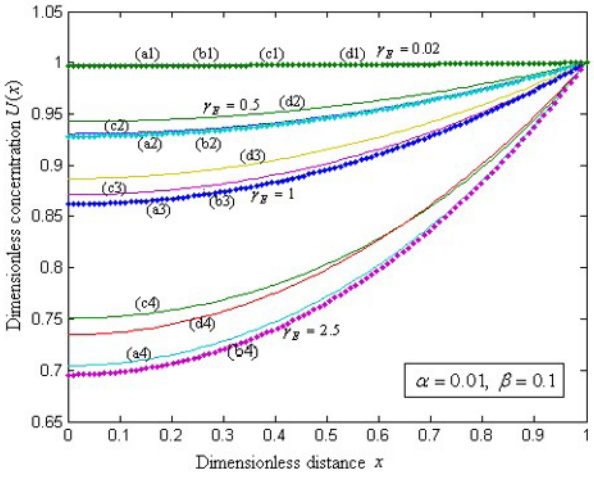

Figure 4.4: Dimensionless concentration $U(x)$ versus dimensionless distance x when α = 0.01, β = 0.1. The curves a1, a2, a3, a4 (ADM), b1, b2, b3, b4 (simulation), c1, c2, c3, c4 (HAM), d1, d2, d3, d4 (HPM) are plotted when γ_E = 0.2, 0. 5, 1, 2. 5 Symbols (---) equations. (4.10)-(4.12) and (…) numerical simulation.

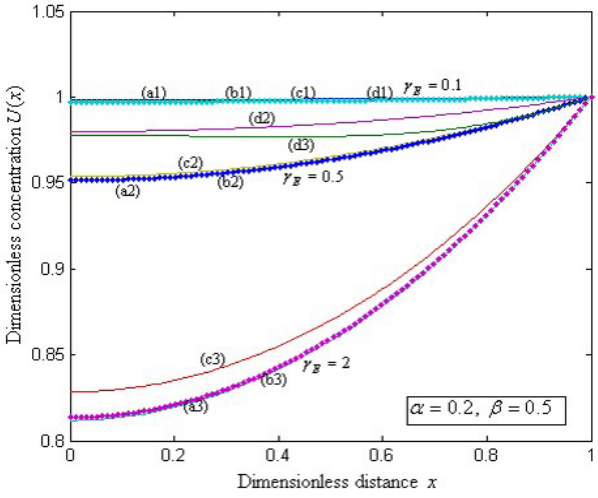

Figure 4.5: Dimensionless concentration $U(x)$ versus dimensionless distance x when α = 0.2, β = 0.5. The curves a1, a2, a3 (ADM), b1, b2, b3 (simulation), c1, c2, c3 (HAM), d1, d2, d3 (HPM) are plotted when γ_E = 0.1, 0.5, 2. Symbols (---) equations (4.10)-(4.12) and (…) numerical simulation.

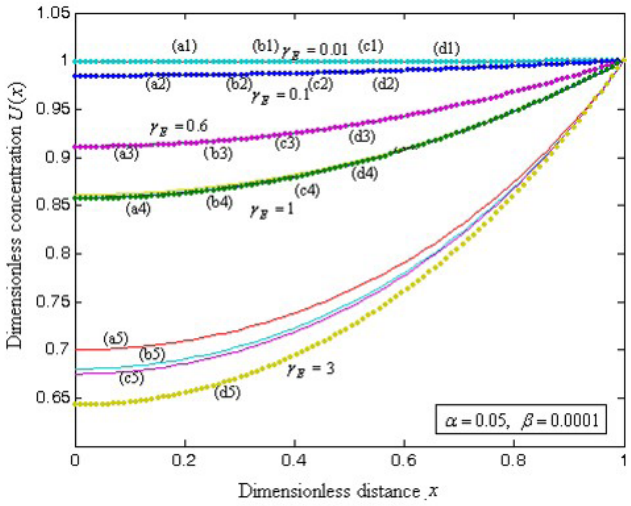

Figure 4.6: Dimensionless concentration $U(x)$ versus dimensionless distance x when α = 0.05, β = 0.0001. The curves a1, a2, a3, a4, a5 (HPM), b1, b2, b3, b4, b5 (HAM), c1, c2, c3, c4, c5 (ADM), d1, d2, d3, d4, d5 (simulation) are plotted when γ_E = 0.01, 0.1, 0.6, 1,3 Symbols (---) equations. (4.10)-(4.12) and (…) numerical simulation.

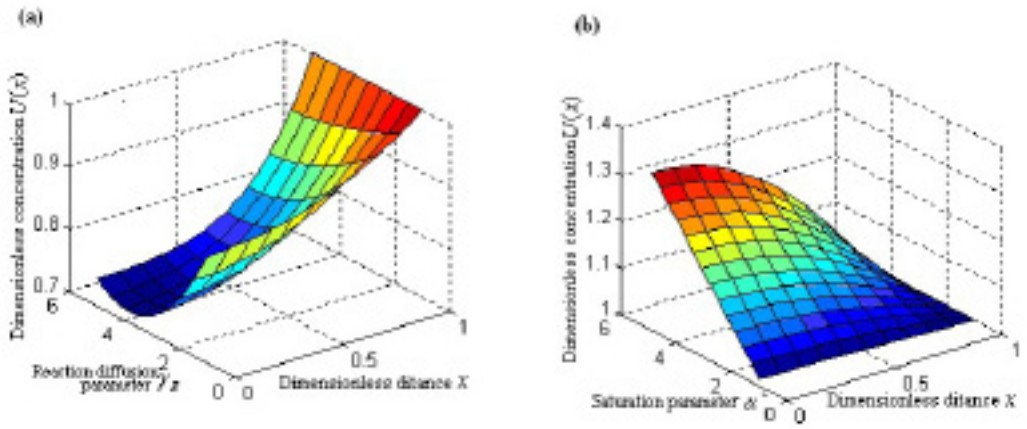

Figure 4.7: The normalized three dimensionless steady-state concentration profiles $U(x)$ calculated using equation (4.10) .The plot was constructed for the values of and $\alpha = 0.1$ *and* $\beta = 0.001$, *and* $\gamma_E = 0.01$.

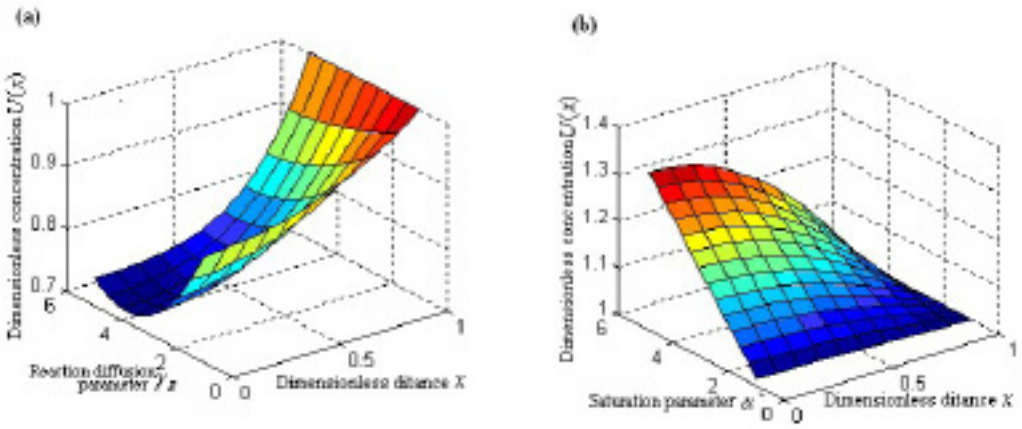

Figure 4.8: The normalized three dimensionless steady-state concentration profiles $U(x)$ calculated using equation (4.11) .The plot was constructed for the values of $\alpha = 0.1$ *and* $\beta = 0.001$, *and* $\gamma_E = 0.1$.

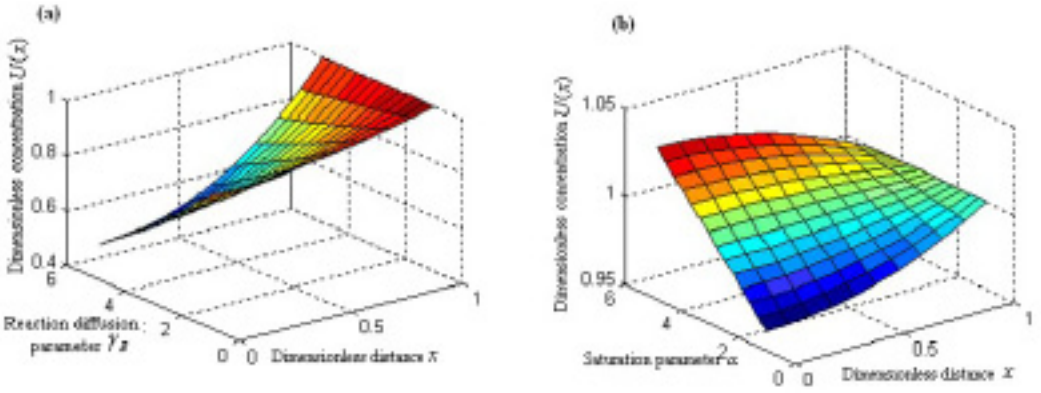

Figure 4.9: The normalized three dimensionless steady-state concentration profiles $U(x)$ calculated using equation (4.12). The plot was constructed for the values of $\alpha = 0.1$ *and* $\beta = 0.001$, *and* $\gamma_E = 0.1$.

4.8. Conclusion

A non-linear ordinary differential equation in the investigation of kinetics of immobilized liver esterase by flow calorimetry has been solved using Adomian decomposition method, Homotopy analysis and Homotopy perturbation method. The simple approximate expression of concentration of substrate for all values of parameters α, β and γ_E are reported. These methods can be easily extended to find the solution of all other non-linear reaction diffusion equations for immobilized enzymes with reversible Michaelis-Menten kinetics for various complex boundary conditions. These analytical results are useful for design and optimization of immobilized liver esterase by flow calorimetry.

4.9. Appendix 4.A

Basic concept of the Adomian decomposition method (ADM)

Adomian decomposition method [9-13] depends on the non-linear differential equation

$$F(x, y(x)) = 0 \tag{4.A1}$$

into the two components

$$L(y(x)) + N(y(x)) = 0 \tag{4.A2}$$

where L and N are the linear and non-linear parts of F respectively. The operator L is assumed to be an invertible operator. Solving for $L(y)$ leads to

$$L(y) = -N(y) \tag{4.A3}$$

Applying the inverse operator L on both sides of equation (4.A3) yields

$$y = -L(N(y)) + \varphi(x) \tag{4.A4}$$

where φ(x)is the constant of integration which satisfies the condition L(φ) Now assum-

ing that the solution y can be represented as infinite series of the form

$$y = \sum_{n=0}^{\infty} y_n \tag{4.A5}$$

Furthermore, suppose that the non-linear term $N(y)$ can be written as infinite series in terms of the Adomian polynomials A_n of the form

$$N(y) = \sum_{n=0}^{\infty} A_n \tag{4.A6}$$

where the Adomian polynomials A_n of $N(y)$ are evaluated using the formula:

$$A_n(x) = \frac{1}{n!}\frac{d^n}{d\lambda^n} N\left(\sum_{n=0}^{\infty} \lambda^n y_n\right)\Big|_{\lambda=0} \tag{4.A7}$$

Then substituting equations. (4.A5) and (4.A6) in equation (4.A4) gives

$$\sum_{n=0}^{\infty} y_n = \varphi(x) - L^{-1}\left(\sum_{n=0}^{\infty} A_n\right) \tag{4.A8}$$

Then equating the terms in the linear system of equation (4.A8) gives the recurrent relation

$$y_0 = \varphi(x),\ y_{n+1} = -L^{-1}(A_n) \qquad L^{\ 1} \tag{4.A9}$$

However, in practice all the terms of series in equation. (4.A7) cannot be determined, and the solution is approximated by the truncated series $\sum_{n=0}^{\infty} y_n$. This method has been proven to be very efficient in solving various types of non-linear boundary and initial value problems.

4.10. Appendix 4.B

Analytical solutions of concentrations of substrate using ADM

In this appendix, we derive the general solution of nonlinear equation (4.7) by using Adomian decomposition method. We write the equation (4.7) in the operator form,

$$L(U) = \frac{\gamma_E U}{1 + \alpha U + \beta U^2} \tag{4.B1}$$

where $L = x^{-1}\dfrac{d^2}{dx^2}x$. Applying the inverse operator L^{-1} on both sides of equation. (4.B1) yields

$$U(x) = A + \frac{B}{x} + \gamma_E L^{-1}\left(\frac{U}{1 + \alpha U + \beta U^2}\right) \tag{4.B2}$$

where A and B are the constants of integration. We let,

$$U(x) = \sum_{n=0}^{\infty} U_n(x) \tag{4.B3}$$

$$N[U(x)] = \sum_{n=0}^{\infty} A_{\mathrm{n}} \tag{4.B4}$$

where $$N[U(x)] = \left(\frac{U}{1 + \alpha U + \beta U^2} \right) \tag{4.B5}$$

In view of equations (4.B3 - B5), equation (4.B 2) gives

$$\sum_{n=0}^{\infty} U_n(x) = A + \frac{B}{x} + \gamma_E L^{-1} \sum_{n=0}^{\infty} A_{\mathrm{n}} \tag{4.B6}$$

We identify the zeroth component as

$$U_0(x) = A + \frac{B}{x} \tag{4.B7}$$

and the remaining components as the recurrence relation

$$U_{n+1}(x) = \gamma_E L^{-1} A_{\mathrm{n}} \quad n \geq 0 \tag{4.B8}$$

where A_{n} are the Adomian polynomials of $U_1, U_2, ..., U_n$. We can find the first few A_{n} as follows:

$$A_0 = N(U_0) = \frac{1}{1 + \alpha + \beta} \tag{4.B9}$$

$$A_1 = \frac{d}{d\lambda}\left[N(U_0 + \lambda U_1)\right] = \frac{U_1(1-\beta)}{(1+\alpha+\beta)^2} \tag{4.B10}$$

The remaining polynomials can be generated easily, and so,

$$U_0 = 1 \tag{4.B11}$$

$$U_1(x) = \frac{\gamma_E (x^2 - 1)}{6(1 + \alpha + \beta)} \tag{4.B12}$$

$$U_2(x) = \frac{{\gamma_E}^2 (1-\beta)}{6(1+\alpha+\beta)^3} \left(\frac{x^4}{20} - \frac{x^2}{6} + \frac{7}{60}\right) \tag{4.B13}$$

Adding (4.B11) to (4.B13) we get equation (4.11) in the text.

4.11. Appendix 4.C

Approximate analytical solutions of the system of equations (4.7-4.9) using HAM

In this appendix, we indicate how equation (4.11) in this chapter is derived. The Homotopy analysis method was constructed to determine the solution of equations (4.7-4.9).

$$\frac{d^2U}{dx^2} + \frac{2}{x}\frac{dU}{dx} = \frac{\gamma_E U}{1 + \alpha U + \beta U^2} \tag{4.C1}$$

In order to solve equation (4. C1)) by means of the HAM, we first construct the zeroth-order deformation equation by taking $H(t) = 1$,

$$(1-p)\left(\frac{d^2U}{dx^2} + \frac{2}{x}\frac{dU}{dx}\right) = ph\left[\left(\frac{d^2U}{dx^2} + \frac{2}{x}\frac{dU}{dx}\right) + \alpha U\left(\frac{d^2U}{dx^2} + \frac{2}{x}\frac{dU}{dx}\right) + \beta U^2\left(\frac{d^2U}{dx^2} + \frac{2}{x}\frac{dU}{dx}\right) - \gamma_E U\right] \tag{4. C2}$$

The approximate solutions of equation (4. C2) are as follows

$$U = U_0 + pU_1 + p^2U_2 + p^3U_3 + ... \tag{4. C3}$$

Substituting the series (4. C3) in equation (4. C2) and equating the like powers of p we get

$$p^0 : \frac{d^2U_0}{dx^2} + \frac{2}{x}\frac{dU_0}{dx} = 0 \tag{4.C4}$$

$$p^1 : \frac{d^2U_1}{dx^2} + \frac{2}{x}\frac{dU_1}{dx} = (h+1)\left(\frac{d^2U_0}{dx^2} + \frac{2}{x}\frac{dU_0}{dx}\right) + h\alpha U_0\left(\frac{d^2U_0}{dx^2} + \frac{2}{x}\frac{dU_0}{dx}\right) + h\beta {U_0}^2\left(\frac{d^2U_0}{dx^2} + \frac{2}{x}\frac{dU_0}{dx}\right) - h\gamma_E U_0 \tag{4. C5}$$

$$p^2 : \frac{d^2U_2}{dx^2} + \frac{2}{x}\frac{dU_2}{dx} = (h+1)\left(\frac{d^2U_1}{dx^2} + \frac{2}{x}\frac{dU_1}{dx}\right) + h\alpha U_0\left(\frac{d^2U_1}{dx^2} + \frac{2}{x}\frac{dU_1}{dx}\right) + h\beta {U_0}^2\left(\frac{d^2U_1}{dx^2} + \frac{2}{x}\frac{dU_1}{dx}\right) + h\alpha U_1\left(\frac{d^2U_0}{dx^2} + \frac{2}{x}\frac{dU_0}{dx}\right) + 2h\beta U_0U_1\left(\frac{d^2U_0}{dx^2} + \frac{2}{x}\frac{dU_0}{dx}\right) - h\gamma_E U_1 \tag{4. C6}$$

The boundary conditions becomes

$$U_0(x=1) = 1, \quad \frac{dU_0(x=0)}{dx} = 0 \tag{4.C7}$$

and

$$U_i(x=1) = 0, \quad \frac{dU_i(x=0)}{dx} = 0 \qquad \forall i = 1,2,3,... \tag{4.C.8}$$

Now applying the boundary conditions equation (4.C7) in equation (4.C4) we get

$$U_0(x) = 1 \tag{4.C9}$$

Substituting the values of U_0 in equation (4.C5) and solving the equation using the boundary conditions equation (4.C8) we obtain the following result:

$$U_1(x) = \frac{h\gamma_E}{6}(1-x^2) \tag{4.C10}$$

Substituting the values of U_0 and U_1 in equation (4.C6) and solving the equation using the boundary conditions equation (4.D8) we obtain the following result:

$$U_2(x) = \frac{h\gamma_E}{6} + \frac{h^2\gamma_E}{6}(1+\alpha+\beta) - (1+\alpha+\beta)\frac{h^2\gamma_E x^2}{6} - \frac{h\gamma_E x^2}{6} + \frac{h^2{\gamma_E}^2}{6}\left(\frac{x^4}{20} - \frac{x^2}{6} + \frac{7}{60}\right) \tag{4.D11}$$

To find few iteration we get, the solution of $U(x)$ to reach the better approximation. Adding (4.C9), (4.C10) and (4.C11), we get equation (4.11) in the text.

4.12. Appendix 4. D

Approximate analytical solutions of the system of equations (4.7-4.9) using HPM

Solution of the equations (4.7-4.9) using Homotopy perturbation method. In this appendix, we indicate how equation. (4.12) in this chapter is derived. Furthermore, a Homotopy was constructed to determine the solution of equation (4.7).

$$(1-p)\left(\frac{d^2U}{dx^2}+\frac{2}{x}\frac{dU}{dx}\right)+p\left[(1+\alpha U+\beta U^2)\left(\frac{d^2U}{dx^2}+\frac{2}{x}\frac{dU}{dx}\right)-\gamma_E U\right]=0 \tag{4.D1}$$

The approximate solutions of equation (4.D1) is

$$U=U_0+pU_1+p^2U_2+p^3U_3+... \tag{4.D2}$$

Substituting equation (4.D2) into equation (4.D1), and comparing the coefficients of like powers of p

$$p^0:\frac{d^2U_0}{dx^2}+\frac{2}{x}\frac{dU_0}{dx}=0, \tag{4.D3}$$

$$p^1:\left(\frac{d^2U_1}{dx^2}+\frac{2}{x}\frac{dU_1}{dx}\right)+\alpha U_0\left(\frac{d^2U_0}{dx^2}+\frac{2}{x}\frac{dU_0}{dx}\right)+\beta U_0^2\left(\frac{d^2U_0}{dx^2}+\frac{2}{x}\frac{dU_0}{dx}\right)-\gamma_E U_0=0, \tag{4.D4}$$

$$p^2:\left(\frac{d^2U_2}{dx^2}+\frac{2}{x}\frac{dU_2}{dx}\right)+\alpha U_1\left(\frac{d^2U_0}{dx^2}+\frac{2}{x}\frac{dU_0}{dx}\right)+\alpha U_0\left(\frac{d^2U_1}{dx^2}+\frac{2}{x}\frac{dU_1}{dx}\right)+\beta U_0^2\left(\frac{d^2U_1}{dx^2}+\frac{2}{x}\frac{dU_1}{dx}\right) \tag{4.D5}$$
$$2\beta U_0U_1\left(\frac{d^2U_0}{dx^2}+\frac{2}{x}\frac{dU_0}{dx}\right)-\gamma_E U_1=0,$$

The boundary conditions are

$$U_0(x=1)=1,\quad \frac{dU_0(x=0)}{dx}=0 \tag{4.D6}$$

and

$$U_i(x=1)=0,\quad \frac{dU_i(x=0)}{dx}=0 \qquad \forall i=1,2,3,... \tag{4.D7}$$

Solving the equations (4.D3) to (4.D5) and using the boundary conditions (4.D6) and (4.D7), we can find the following results

$$U_0(x)=1 \tag{4.D8}$$

$$U_1(x)=\frac{\gamma_E(x^2-1)}{6} \tag{4.D9}$$

$$U_2(x)=\frac{\gamma_E}{6}\left(\frac{7\gamma_E}{60}+\alpha+\beta\right)-\left(\frac{\gamma_E}{6}+\alpha+\beta\right)\frac{\gamma_E x^2}{6}+\frac{\gamma_E^2x^4}{120} \tag{4.D10}$$

According to the HPM, we can conclude that

$$U(x)=\lim_{p\to 1}U(x)=U_0(x)+U_1(x)+U_2(x)+.... \tag{4.D11}$$

Using equations (4.D8), (4.D9) and (4.D10) in equation. (4.D11), we obtain the final

results are described in equation (4.12).

4.13. Appendix 4.E

In this appendix, we derive the solution of equation (4.D4) by using reduction of order. To illustrate the basic concepts of reduction of order, we consider the equation

$$\frac{d^2c}{dx^2} + P\frac{dc}{dx} + Qc = R \tag{4.E1}$$

where *P, Q,, R* are function of x. Equation (4.D4) can be simplified to

$$\frac{d^2U_2}{dx^2} + \frac{2}{x}\frac{dU_2}{dx} = \frac{\gamma_E^2(x^2-1)}{6} - \alpha\gamma_E - \beta\gamma_E \tag{4.E2}$$

Using reduction of order, we have

$$P = \frac{2}{x};\quad Q = 0;\quad R = \frac{\gamma_E^2(x^2-1)}{6} - \alpha\gamma_E - \beta\gamma_E \tag{4.E3}$$

Let $U_2 = wv$ (4.E4)

Substitute (4.E4) in (4.E1), if U_2 is so chosen that

$$2\frac{dw}{dx} + Pw = 0 \tag{4.E5}$$

Substituting the value of P in the above equation (4.E5) becomes

$$w = \frac{1}{x} \tag{4.E6}$$

The given equation (4.E2) reduces to

$$v'' + Q_1 v = R_1 \tag{4.E7}$$

where

$$Q_1 = Q - \frac{P^2}{4} + \frac{P'}{2} = 0,\quad R_1 = \frac{R}{c} \tag{4.E8}$$

Substituting (4.E8) in (4.E7) we obtain,

$$v'' = \frac{\gamma_E^2(x^3-x)}{6} - \alpha\gamma_E x - \beta\gamma_E x \tag{4.E9}$$

Integrating equation (4.E9) twice, we obtain

$$v = Ax + B + \frac{\gamma_E^2}{6}\left(\frac{x^5}{20} - \frac{x^3}{6}\right) - \alpha\gamma_E\frac{x^3}{6} - \beta\gamma_E\frac{x^3}{6} \tag{4.E10}$$

Substituting (4.E6) and (4.E10) in (4.E4) we have,

$$U_2 = A + \frac{B}{x} + \frac{\gamma_E^2}{6}\left(\frac{x^4}{20} - \frac{x^2}{6}\right) - \alpha\gamma_E\frac{x^2}{6} - \beta\gamma_E\frac{x^2}{6} \tag{4.E11}$$

Using the boundary conditions equations (4.D6) and (4.D7), we can obtain the value of

the constants A and B. Substituting the value of the constants A and B in the equation (4.E11) we obtain the equation (4.D10). Similarly we can solve the other differential equations (4.B11), (4.C4), (4.C5), (4.C6), (4.E3) and (4.E5) using the reduction of order method.

4.14. Appendix 4.F

Scilab/Matlab program to find the numerical solution of equations (4.7-4.9).

```
function pdex1
m = 2;
x = linspace(0,1);
t = linspace(0,100);
sol = pdepe(m,@pdex1pde,@pdex1ic,@pdex1bc,x,t);
u = sol(:,:,1);
surf(x,t,u)
title('Numerical solution computed with 20 mesh points.')
xlabel('Distance x')
ylabel('Time t')
figure
plot(x,u(end,:))
title('Solution at t = 2')
xlabel('Distance x')
ylabel('u(x,2)')
% --------------------------------------------------------------
function [c,f,s] = pdex1pde(x,t,u,DuDx)
c = 1;
f = DuDx;
r=10;
alpha=5;
beta=2;
s = -r*u/(1+alpha*u+beta*u*u);
% --------------------------------------------------------------
function u0 = pdex1ic(x)
u0 = 1;
% --------------------------------------------------------------
function [pl,ql,pr,qr] = pdex1bc(xl,ul,xr,ur,t)
pl = 0;
ql = 1;
pr = ur-1;
qr = 0;
```

4.15. Appendix 4.G

Determining the region of *h* for validity

The analytical solution should converge. It should be noted that the auxiliary parameter *h* controls the convergence and accuracy of the solution series. The analytical solution represented by equation (4.11) contains the auxiliary parameter *h*, which gives the convergence region and rate of approximation for the Homotopy analysis method. In order to define region such that the solution series is independent of *h*, a multiple of *h*-curves are plotted. The region where the distribution of $U(x)$ and $U'(x)$ versus *h* is a horizontal line is known as the convergence region for the corresponding function. The common region among $U(x)$ and its derivatives are known as the over all convergence region. To study the influence of *h* on the convergence of solution, the *h*-curves of $U(0.5)$ and $U'(0.5)$ are plotted in figure 4.2(a), figure 4.2(b) respectively, for $\alpha = 0.5, \beta = 0.3, \gamma_E = 0.5$. These figures clearly indicate that the valid region of *h* is about (-2 to -0.5). Similarly we can find the value of the convergence control parameter *h* for different values of constant parameters.

4.16. Appendix 4.H

Nomenclature and Units.

Symbol	Meaning	Usual dimension
c_{SP}	Substrate concentration	mmoldm^{3}
c_S	Phenyl acetate concentration	mmoldm^{3}
K_i	Substrate inhibition constant	mmoldm^{3}
K_m	Michaelis constant	mmoldm^{3}
V_m	Kinetic parameter	mK
r	Particle radial co-ordinate	None
R_p	Particle radius	None
D_e	Diffusion coefficient	$\mathrm{dm}^2 s^{-1}$
α , β	Saturation parameters	None
x	Dimensionless distance	None
U	Dimensionless concentration	None
γ_E	Reaction diffusion parameter	None

4.17. References

1. P. Monk and I. Wadso,, A Flow Micro Reaction Acta Chem. Scand. 22, 1842-1852, 1968.

2. J. Burch, The purification and properties of horse liver esterase, Biochem. J. 58, 415-426, 1954.

3. J.K. Stoops, D.J. Horgan, M.T.C. Runnegar, J.De Jersey, E.C. webb and B. Zerner, JK, Horgan DJ, Runnegar, MT, De Jersey J, Webb EC, Zerner B. Carboxylesterases Kinetic studies on carboxylesterases. Biochemistry. 8(5):2026-33, 1969.

4. A.J. Adler and G.B. Kistiakowasky, Kinetics of Pig Liver Esterase Catalysis J. Am. Chem. Soc. 84, 695-703, 1962.

5. V.Stefuca, P.Gemenier, and T. Scheper (Ed.) Advances in Biochemical Engineering Biotechnology, Springer, Berlin, Vol. 64 , p.71, 1999

6. V. Stefuca, A. Vikartovska-Welwardova and P.Gemenier, Flow microcalorimeter auto- calibration for the analysis of immobilized enzyme kinetics, Anal. Chim. Acta 355 63, 1999.

7. V. Stefuca, Ingrid Cipakova, Peter Gemeiner,investigation of immobilized glucoamylase kinetics by flow calorimetry, Thermochim. Acta 378, 79-85, 2001.

8. F. Malik, V. Stefuca and V. Bales, . Investigation of kinetics of immobilized liver esterase by flow calorimetry J. Mol. Catal. 29, 81-87, 2004.

9. O. K. Jaradat, Adomian decomposition method for solving abelian differential equations J. Appl. Sci. 8, 1962-1966, 2008.

Majid Wazwaz and A. Gorguis, The decomposition method applied to systems of partial differential equations. Applied Mathematics and Compuation 149, 807-814, 2004.

10. O.D. Makinde, Adomian decomposition approach to a SIR epidemic model with constant vaccination strategy, Appl. Math. Comp. 184, 842-848, 2007.

A. M. Siddiqui, M. Hameed, B. M.Siddiqui and Q.K.Ghori, Use of Adomia Decomposition method in the study of parallel plate flow of a third grade fluid Commun. Nonlinear Sci.Numer. Simul. 15, 2388-2399, 2010.

11. M.A. Mohamed, Comparison Differential Transformation Technique with Adomian Decomposition Method for Dispersive Long-wave Equations in (2+1)-Dimensions Appl. Math. 5, 148-166, 2010.

12. S.J. Liao. The proposed homotopy nalysis technique for the solution of nonlinear problems, Ph. D., thesis, Shanghai Jiao Tong University, 1992.

13. S.J. Liao, Beyond Perturbation: Introduction to the Homotopy Analysis Method. 1st Edn.Chapman and Hall, CRC Press, Boca Raton, 2003.

14. F. Awaadeh, H. M. Jaradat and O. Alsyyed. Analytical solution for nonlinear Gas Dynamic equation by Homotopy Analysis Method Chaos. Solitons & fractals, 42, 1422- 1427, 2009.

15. H. Jafari, C. Chun and S. Saeidy, Analytical solution for nonlinear Gas Dynamic Equation by Homotopy Analysis Method Appl. Math. 4, 149-154, 2009

A. R. Sohouli, M. Famouri, A. Kimiaeifar and G. Domairry, Application of homotopy analysis method for natural convection of Darcian fulid about a vertical full cone embedded in pours media prescribed surface heat flux, Commun. Nonlinear Sci. Numer. Simul. 15, 169- 199, 2010.

16. G .Domarriy and M. Fazeli, Homotopy analysis method to determine the fin efficiency of convective straight fins with temperature-dependent thermal conductivity., Comm. Nonlinear Sci. Numer. Simul. 14, 489-499, 2009.

17. S. J. Liao, On the homotopy analysis method for nonlinear problems., Appl. Math. Comput. 147, 499-513, 2004.

18. G. Domairry and H. Barring. An approximation of the analytic solution of some nonlinear heat transfer equations: A survey by using homotopy analysis method., Adv. Studies. Theor. Phys. 2, 507-518, 2008.

19. J. H. He, A coupling method of homotopy technique and a perturbation technique for non-linear problems, Int. J. Nonlinear Mech. 35, 37-43, 2000.

20. D. D. Ganji, M. Amini and A. Kolahdooz, Am. J. Eng. Analytical Investigation of Hyperbolic Equations via He's Methods., American Journal of Engineering and Applied Sciences, 1 (4), 399-407, 2008.

21. P. D. Ariel, homotopy perumbation method and natural convention flow of a third grade fluid through a circular tubenon., Nonlinear Sci. Lett. A., 1, 43-52, 2010.

22. A. Fereidoon, Y. Rostamiyan, M.R. Davoudabadi, S.D. Farahani and D.D. Ganji, Analytic Approach to Investigation of Distributions of Stresses and Radial Displacement at the Thick-wall Cylinder under the Internal and External Pressures., Middle-East Journal of Scientific Research 5 (5), 321-328, 2010.

Boundary Valur Broblem and Behaviour of Porous Catalyst Articles In View of Internal Mass and Heat Diffusion Effects

Chapter 5

5.1. Introduction

The reaction rate in a porous catalyst is affected by intraparticle mass and heat transfer in addition to the intrinsic kinetics. Except for an isothermal first-order reaction and a zero-order reaction, the balance equations are non-linear and are usually solved numerically to calculate the effectiveness factor. Since the numerical solution of the problem is regarded as tedious and time consuming, approximation of the effectiveness factor has been extensively investigated in the past and various simple approximate formulae are available in textbooks (for example, [1-5]).

The usual numerical methods for the boundary-value problem are the finite-difference methods, the shooting methods [6] and the orthogonal collocation methods [7]. When the problem is non-linear, the methods become necessarily iterative ones, finding an improved solution based on the results of the previous iterations with a prospect that the iterative procedure will lead to the desired solution. The finite-difference method converts the boundary-value problem to a system of non-linear algebraic equations, the solution of which can be very difficult to obtain, especially when many base points are used in the method. The collocation methods are efficient when successful, but they are often unstable when many collocation points are used and the Thiele modulus is large [8]. The shooting methods convert the boundary-value problem into an initial-value problem, in which the missing boundary condition at the initial point is assumed. Through an iterative procedure, the methods try to produce a solution that agrees with all the given boundary conditions [9].

An interval method [10], continuation method [11], a branch and bound algorithm [12], simulated annealing [13], genetic algorithms [14], a terrain-following method [15,16] are also used to solve the non-linear equations. Currently, both trial-and-error shooting method [17, 18] and a direct method that combines numerical integration and interval analysis [19] are available to find all solutions. Angelo Lucia [20] and co-workers present the two different collocation methods for the classical reaction –transport problems in spherical catalyst pellet. However, to the best of our knowledge, there was no rigorous solution for the concentration of reactant A at the surface of catalyst has been reported. The purpose of this chapter is to derive simple analytical expression for concentration and effectiveness factor for all possible values of reaction/diffusion parameters γ , β *and* ϕ.

5.2. Reaction and diffusion in catalyst Pellets.

Many industrial reactors involve heterogeneous reaction kinetics of packed catalytic pellets in fixed-bed reactors, as illustrated in equation (1). A single catalyst pellet of radius *R* can be treated as a porous medium through which reactants diffuse while reactions occur simultaneously.

$$A \xrightarrow[\nabla H]{catalyst} B \tag{5.1}$$

The species and energy balances for diffusive transport inside the pellet can be written as follows [21]:

$$D_{\varepsilon}\nabla^2 C_A + r_A = 0 \tag{5.2}$$

$$K_{\varepsilon}\nabla^2 T + r_A \Delta H = 0 \tag{5.3}$$

Equation (5.2) is represent species balance and equation (5.3) is represent the heat balance.

Where Arrhenius reactions rate is $$r_A = -k_{ref}\exp\left[\frac{-E}{R_g T_{ref}}\left(\frac{T_{ref}}{T_s}-1\right)\right]C_{A,s} \tag{5.4}$$

The boundary conditions are

$$C_A\big|_{r=R} = C_{A,s} \tag{5.5}$$

$$T\big|_{r=R} = T_s \tag{5.6}$$

$$\nabla C_A\big|_{r=0} = \nabla T\big|_{r=0} = 0 \tag{5.7}$$

At the surface, concentration and temperature can be given by a Dirichlet boundary condition such as that in equations (5.5) and (5.6). Because of symmetry, the mass and energy flux at the center of the catalyst pellet is zero, as shown in equation (5.7). The system described by equations (5.2)-(5.7) represents the nonlinear PDE system for coupled heat and mass transfer in a spherical non-isothermal catalyst pellet. After inserting the temperature profile into the species balance, equations (5.2)-(5.7) can be written in terms of the dimensionless concentration *y* ($y = C_A/C_A$,s), the dimensionless pellet radius *x* ($x = r/R$), and dimensionless constants α, β and ϕ. Using this dimensionless variable dimensionless non-isothermal species and heat transport are as follows [22]:

$$\frac{d^2 y}{dx^2} + \frac{2}{x}\frac{dy}{dx} - \phi^2 y \exp\left[\frac{\gamma\beta(1-y)}{1+\beta(1-y)}\right] = 0 \tag{5.8}$$

The parameters ϕ, ã and â are in equation (5.8) represent the dimensionless activation energy, the dimensionless heat of reaction, and the Thiele modulus as evaluated at the surface of the spherical catalyst pellet, respectively. These parameters are expressed in terms of the

pellet transport and reaction properties, as well as the pellet surface concentration ($C_{A,S}$) and (T_S) as follows:

$$\phi = R\left\{\frac{k_{ref}}{D}\exp\left[\frac{-E}{RgT_{ref}}\left(\frac{T_{ref}}{T_s}-1\right)\right]\right\}^2 \quad (5.9)$$

$$\gamma = \frac{E}{R_g T_s} \quad (5.10)$$

$$\beta = \frac{-\Delta H D_{\varepsilon z}}{K_{\varepsilon z}}\left(\frac{C_{A,S}}{T_S}\right) \quad (5.11)$$

where C_A is the concentration of reactant A inside the catalyst pellet, $C_{A,s}$ is the concentration of reactant A at the surface of catalyst pellet, $D_{\varepsilon z}$ is the effective diffusivity inside the catalyst pellet, is the activation energy, Δ is th heat of reaction, k_{ref} is the reference reaction constant, $K_{\varepsilon z}$ is the effective thermal conductivity inside the catalyst pellet, r_A is the arrhenius reaction rate, R_g is the universal gas constant, T is the temperature inside the catalyst pellet, T_{ref} is the reference temperature and T_s is the temperature at the surface of catalyst pellet. The boundary conditions in dimensionless forms are

$$y\big|_{x=1} = 1 \quad (5.12)$$

$$\frac{dy}{dx}\Big|_{x=0} = 0 \quad (5.13)$$

The overall reaction rate in a catalytic pellet is often expressed by the effectiveness factor (η), which measures the total reaction rate as a scalar multiple of a homogeneous first-order reaction at the surface concentration. The effectiveness factor for spherical pellet is [23]:

$$\eta = \frac{3}{\phi^2}\frac{dy}{dx}\Big|_{x=1} \quad (5.14)$$

5.3. Analytical solution of the concentration using modified Adomian decomposition method (MADM)

In the recent years, much attention is devoted to the application of the Adomian decomposition method to the solution of various scientific models [24]. An efficient modification of the standard Adomian decomposition method for solving singular initial value problem in the second order partial differential equation. The MADM yields, without linearization, perturbation, transformation or discretisation, an analytical solution in terms of a rapidly convergent infinite power series with easily computable terms. The decomposition method is simple and easy to use and produces reliable results with few iterations used. The results show that the rate of convergence of modified Adomian decomposition method is higher than standard Adomian decomposition method [25-29]. Using this method (see Appendix 5.A), we can obtain the analytical expression of concentration (see Appendix 5.B), of the substrate as follows:

$$y(x) = 1 - \frac{\phi^2}{6} + \frac{7}{360}\phi^4(1-\gamma\beta) + \phi^2\left(\frac{1}{6} - \frac{\phi^2(1-\gamma\beta)}{36}\right)x^2 + \frac{\phi^4(1-\gamma\beta)}{120}x^4 \quad (5.15)$$

Using equqtion. (5.10), we can obtain the effectiveness factor

$$\eta = 1 - \frac{\phi^2(1-\gamma\beta)}{15} \quad (5.16)$$

The equations (5.14) and (5.15) represent the new and simple analytical expression of concentration of substrate and effectiveness factor.

5.4. Numerical simulation

The non linear diffusion equation (5.8) for the boundary conditions (equations (5.12) and (5.13)) is also solved numerically. We have used the function pdex1 in MATLAB software to solve numerically the initial-boundary value problems for the nonlinear differential equations. This numerical solution is compared with our analytical results in figures 5.1 and 5.2. Upon comparison, it gives a satisfactory agreement for all values of the dimensionless parameters, α, β and ϕ. The MATLAB program is also given in Appendix 5.*C*.

5.5. Discussion

The nonlinear PDE system for coupled heat and mass transfer in a spherical non-isothermal catalyst pellet is solved analytically. The concentration of substrate depends on the following there factors, γ (dimensionless activation energy), β (dimensionless heat of reaction) and ϕ (Thiele modulus). Figure 5.1(a)-(*b*) shows the dimensionless concentration y versus dimensionless pellet radius x. The concentrations were computed for various values of the dimensionless parameter γ, β and ϕ. From figures 5.1(a)-(b), it is evident that the value of concentration $y \approx 1$ when $x = 1$ and $\phi \leq 0.5$ for all values of γ and β. The concentration y decreases when ϕ increases.

The normalized numerical simulation of three dimensional substrate concentrations y versus dimensionless pellet radius x is shown in figures 5.2(a)-(c)**.** For fixed value of β (= 0.1) the value of concentration $y(x)$ is slowly decreasing when ϕ is increasing. Then the concentration of $y(x)$=1 when $x = 1$ and for all values of ϕ, γ and β. In these figure, it should be noted that the value of the concentration of substrate decreases for all values of γ. From this Figures, it is apparent that the value of the concentration of substrate increases when β increases.

The variation in effectiveness factor for various values of γ, β and ϕ using equation (5.12) is shown in Figures 5.3- 5.5. From figure 5.3, it is evident that the effectiveness factor increases with the increasing value of the dimensionless parameter β. From figure 5.4, it is evident that the effectiveness factor increases with the increasing value of the dimensionless

parameter γ. From Figure 5.5, it is evident that the effectiveness factor increases with the increasing value of the dimensionless paramete γ, β. The effectiveness factor is equal to one when for ϕ <0.2 and all values parameters β and γ.

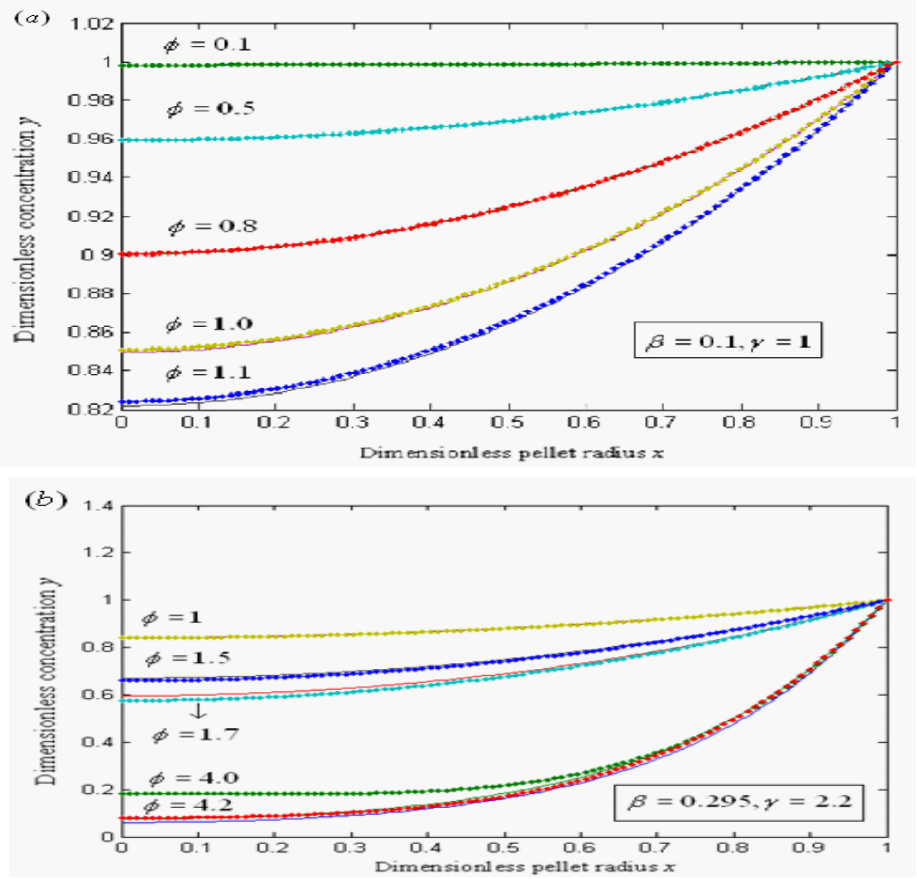

Figure 5.1: Plot of dimensionless concentration $_A$versus dimensionless pellet radius x. The concentrations were computed for various values of the dimensionless parameter ϕ when *(a) β = 0.1, γ = 1 (b) β = 0.295, γ = 202* The curves are plotted using equation (5.15). (—) denotes the analytical results and (• • •) denotes the numerical simulations.

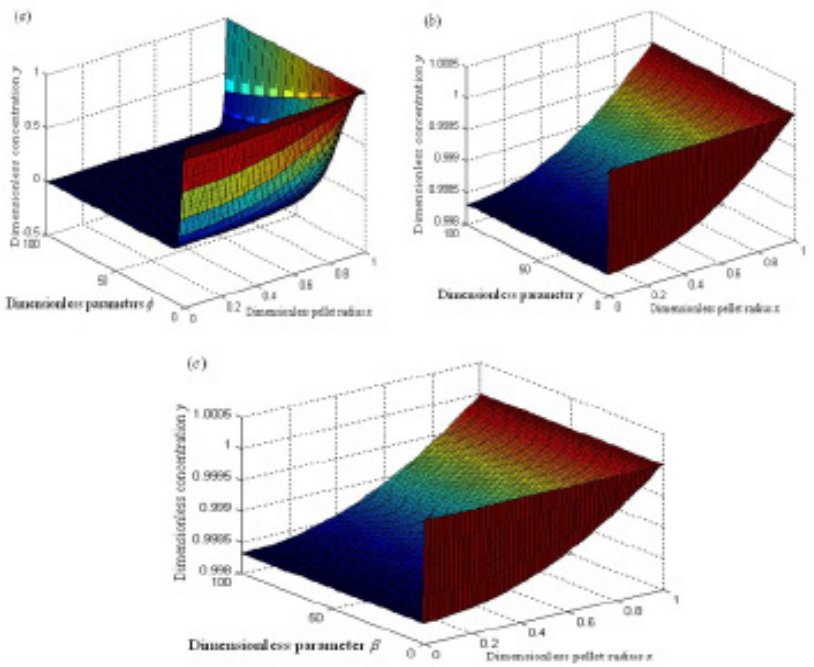

Figure 5.2: The normalized dimensionless concentration $_A$versus dimensionless pellet radius x. calculated using equation. (5.15). The plot was constructed for the values of *(a) β = 0.1, γ = 0.1 (b)* ϕ*= 0.1, β = 0.1 and (c)* ϕ*= 0.1, γ = 0.1.*

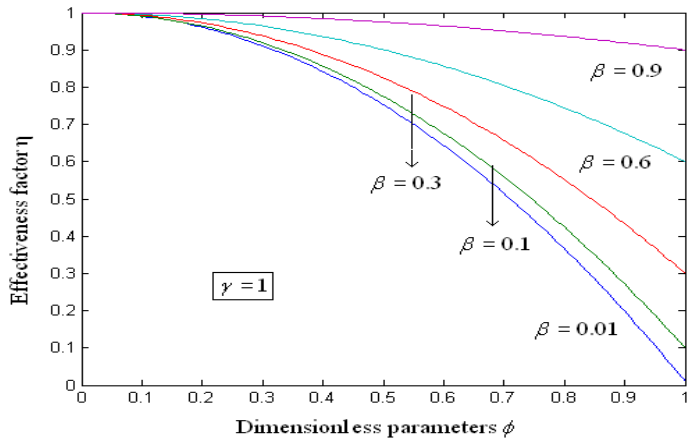

Figure 5.3: Plot of the effectiveness factor η versus dimensionless parameter β. The effectiveness factor η were computed using equation (5.16) when $\gamma = 0.1$.

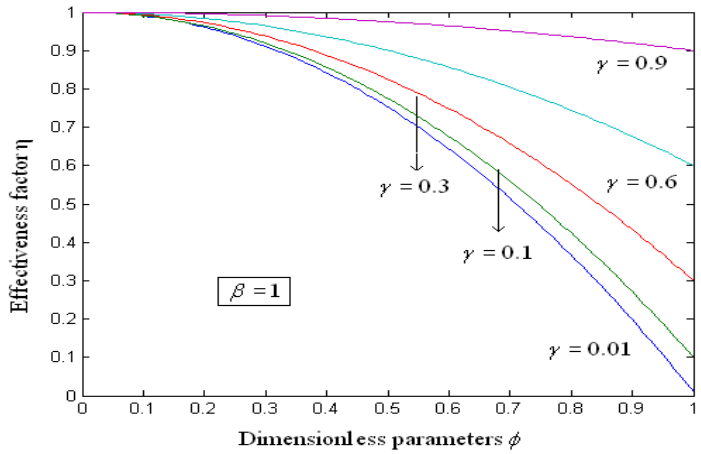

Figure 5.4: Plot of the effectiveness factor η versus dimensionless parameter γ. The effectiveness factor η were computed using equation (5.16) when $\beta = 1$.

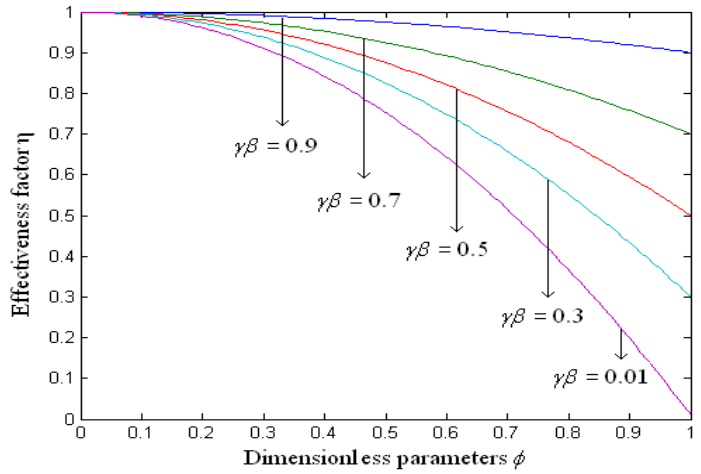

Figure 5.5: Plot of the effectiveness factor η versus dimensionless parameter $_{\gamma\beta}$. The effectiveness factor η were computed using equation (5.16).

5.6. Conclusions

The analytical expression of concentration and effectiveness factor of the reactant A inside the catalyst pellets are derived. The approximate analytical expression for the steady

state concentration of substrate for all values of parameters ϕ,γ and β in a packed bed reactor was obtained using the modified Adomian decomposition method. A satisfactory agreement with the numerical result is noted. Moreover, we have also presented a closed form expression for the effectiveness factor. These analytical results are useful to analyze the reactivity behaviour of porous catalyst particles subject to both internal mass concentration gradients as well as temperature gradients, in endothermic or exothermic reactions.

5.7. Appendix 5.A

Consider the nonlinear differential equation in the form

$$y'' + \frac{2n}{x} y' + \frac{n(n-1)}{x^2} y + F(x, y) = g(x)\,; n \geq 0 \qquad (5.A1)$$

with initial condition

$$y(0) = A,\ y'(0) = B \qquad (5.A2)$$

Where $F(x, y)$ is a real function, $g(x)$ is the given function and A and B are constants. We propose the new differential operator, as below

$$L = x^{-n} \frac{d^2}{dx^2} x^n y \qquad (5.A3)$$

So, the problem (5.A.1) can be written as,

$$Ly = g(x) - F(x, y). \qquad (5.A4)$$

The inverse operator L^{-1} is therefore considered a two-fold integral operator, as below.

$$L^{-1}(.) = x^{-n} \int_0^x \int_0^x x^n\ (.)\, dx\, dx \qquad (5.A5)$$

Applying L^{-1} of (5.A5) to the first three terms $y'' + \frac{2n}{x} y' + \frac{n(n-1)}{x^2} y$ of equation (5.A1) we find

$$L^{-1}\left(y'' + \frac{2n}{x} y' + \frac{n(n-1)}{x^2} y \right) = x^{-n} \int_0^x \int_0^x x^n \left(y'' + \frac{2n}{x} y' + \frac{n(n-1)}{x^2} y \right) dx\, dx$$
$$= x^{-n} \int_0^x (x^n y' + n x^{n-1} y)\, dx$$
$$= y - y(0)$$

By operating L^{-1} on (5.A4), we have

$$y(x) = A + L^{-1} g(x) - L^{-1} F(x, y) \qquad (5.A6)$$

The Adomian decomposition method introduce the solution $y(x)$ and the nonlinear function $F(x, y)$ by infinity series

$$y(x) = \sum_{n=0}^{\infty} y_n(x), \tag{5.A7}$$

$$F(x,y) = \sum_{n=0}^{\infty} A_n \tag{5.A8}$$

where the components $y_n(x)$ of the solution $y(x)$ will be determined recurrently and the Adomian polynomials A_n of $F(x,y)$ are evaluated [24- 26] using the formula

$$A_n(x) = \frac{1}{n!}\frac{d^n}{d\lambda^n} N\left(\sum_{n=0}^{\infty}(\lambda^n y_n)\right)|_{\lambda=0} \tag{5.A9}$$

By substituting (5A7) and (5.A8) into (5.A6),

$$\sum_{n=0}^{\infty} y_n(x) = A + L^{-1}g(x) - L^{-1}\sum_{n=0}^{\infty} A_n \tag{5.A10}$$

Through using Adomian decomposition method, the components $y_n(x)$ can be determined as

$$\begin{aligned} y_0(x) &= A + L^{-1}g(x) \\ y_{n+1}(x) &= -L^{-1}(A_n),\ n \geq 0 \end{aligned} \tag{5.A11}$$

Which gives

$$\begin{aligned} y_0(x) &= A + L^{-1}g(x) \\ y_1(x) &= -L^{-1}(A_0) \\ y_2(x) &= -L^{-1}(A_1) \\ y_3(x) &= -L^{-1}(A_2) \\ &\ldots \end{aligned} \tag{5.A12}$$

From (5.A9) and (5.A12), we can determine the components $y_n(x)$, and hence the series solution of $y(x)$ in (5.A7) can be immediately obtained.

5.8. Appendix 5.B

In this appendix, we derive the general solution of nonlinear equation (5.8) by using Adomian decomposition method. We write the equation (5.8) in the operator form,

$$L(y) = \phi^2 y \exp\left[\frac{\gamma\beta(1-y)}{1+\beta(1-y)}\right] \tag{5.B1}$$

Where $L = x^{-1}\frac{d^2}{d\rho^2}x$. Applying the inverse operator $L^{-1}(.) = x^{-1}\int_0^x\int_0^x x\ (.)\,dx\,dx$ on both sides of Equation (5.B1) yields

$$y(x) = A\,x + B + \phi^2\ L^{-1}\left(y\exp\left[\frac{\gamma\beta(1-y)}{1+\beta(1-y)}\right]\right) \tag{5.B2}$$

where A and *B* are the constants of integration. We let,

$$y(x) = \sum_{n=0}^{\infty} y_n(x) \tag{5.B3}$$

$$N[y(x)] = \sum_{n=0}^{\infty} A_n \tag{5.B4}$$

Where $N[y(x)] = \left(y \exp\left[\frac{\beta (1-y)}{1+\beta(1-y)} \right] \right)$ (5.B5)

In view of Equations (5.B3), (5.B4) and (5.B5), equation (5.B2) gives

$$\sum_{n=0}^{\infty} y_n(x) = A\mathrm{x} + B + \gamma L^{-1} \sum_{n=0}^{\infty} A_n \tag{5.B6}$$

We identify the zeroth component as

$$y_0(x) = A\,x + B \tag{5.B7}$$

$$y_0 = 1 \tag{5.B8}$$

and the remaining components as the recurrence relation

$$y_{n+1}(x) = \phi^2\, L^{-1} A_n \qquad n \geq 0 \tag{5.B9}$$

where A_n are the Adomian polynomials of $y_1, y_2, ..., y_n$. We can find the first few A_n as follows:

$$A_0 = N(y_0) = 1 \tag{5.B10}$$

$$A_1 = \frac{d}{d\lambda}\left[N(y_0 + \lambda y_1)\right] = \frac{\phi^2}{6}(1-\gamma\beta)(x^2-1) \tag{5.B11}$$

The remaining polynomials can be generated easily, and so,

$$y_1 = \frac{\phi^2}{6}(1-\beta)(x^2-1) \tag{5.B12}$$

$$y_2 = \frac{7\phi^4(1-\gamma\beta)}{360} + \phi^4(1-\gamma\beta)\left(\frac{x^4}{120} - \frac{x^2}{36}\right) \tag{5.B13}$$

Adding (5.B8), (5.B12) and (5.B13) we get equation (5.16) in the text.

5.9. Appendix 5.C

The Matlab program to find the numerical solution of equation 8 is as follows.

```
function pdex1

m = 2;
x = linspace(0,1);
t = linspace(0,100);
sol = pdepe(m,@pdex1pde,@pdex1ic,@pdex1bc,x,t);
```

```
u = sol(:,:,1);
surf(x,t,u)
title('Numerical solution computed with 20 mesh points.')xlabel('Distance x')
ylabel('Time t')
figure
plot(x,u(end,:))
title('Solution at t = 2')
xlabel('Distance x')
ylabel('u(x,2)')
% --------------------------------------------------------------
function [c,f,s] = pdex1pde(x,t,u,DuDx)
c = 1;
f = DuDx;
Q=1;
B=1.5;
r=1;
s =-(Q^2)*u*exp(r*B*(1-u)/(1+B*(1-u)));
% --------------------------------------------------------------
function u0 = pdex1ic(x)
u0 = 1;
% --------------------------------------------------------------
function [pl,ql,pr,qr] = pdex1bc(xl,ul,xr,ur,t)
pl = 0;
ql = 1;
pr = ur-1;
qr = 0;
```

5.10. Appendix 4.D

Nomenclature

Symbol	Meaning	Usual dimension
C_A	concentration of reactant A inside the catalyst pellet	cm
$C_{A,s}$	concentration of reactant A at the surface of catalyst pellet	cm
D_ε	Effective diffusivity inside the catalyst pellet	cm^2/s
E	activation energy	kJ mol^{-1}.
g	gradient of $F^T F$	None
ΔH	heat of reaction	kJ mol^{-1}
k_{ref}	reference reaction constant	mmol L^{-1}

K_{ε}	effective thermal conductivity inside the catalyst pellet	mmol L^{-1}
r_A	Arrhenius reaction rate	mmol L^{-1}
R_g	universal gas constant	J/K
T	temperature inside the catalyst pellet	kelvin
T_{ref}	reference temperature	kelvin
T_s	temperature at the surface of catalyst pellet	kelvin
x	dimensionless radius of the spherical catalyst pellet	None
y	dimensionless concentration along radial direction of catalyst pellet	None
β	dimensionless heat of reaction	None
γ	dimensionless activation energy	None
η	effectiveness factor	None
ϕ	Thiele modulus	None

5.11. References

1. G.F. Froment and K. B. Bischoff., Chemical Reactor Analysis and Design, 2nd Edition. Wiley, New York, ., 1990.

2. H.S.Fogler., Elements of Chemical Reaction Engineering, 3rd Edition. Prentice-Hall, Upper Saddle River, New Jersey, 1999.

3. C. G. Jr.Hill., An Introduction to Chemical Engineering Kinetics and Reactor Design. Wiley, New York,1977.

4. R. Aris, The Mathematical Theory of Diffusion and Reaction in Permeable Catalysts. Volume 1. The Theory of the Steady state. Clarendon, Oxford,1975.

5. P. Schneider, , Intraparticle diffusion in multicomponent catalytic reactions. In: Heinemann, H., Carberry, J J. (Eds.)., Catalysis Reviews, Science and Engineering, Vol. 12. Marcel Dekker, New York, pp. 201–278, 1976.

6. B. Carnahan, H. A. Luther and J.O.Wilkes, Applied Numerical Methods. Wiley, New York, 1969.

7. J. Villadsen and M. L. Michelsen., Solution of Differential Equation Models by Polynomial Approximation. Prentice-Hall, Englewood Cliffs, New Jersey, 1978.

8. F. Shiraishi., T. Hasegawa and H. Nagasue,, Accuracy of the numerical solution of a two- point boundary value problem by the orthogonal collocation method. Journal of Chemical Engineering of Japan 28 (3), 316–323, 1995.

9. H. Miyakawa,, H. Nagasue and F. Shiraishi., A highly accurate numerical method for calculating apparent kinetic parameters of immobilized enzyme reactions: 1. Theory. Biochemical Engineering Journal 3 (2), 91–101, 1999

10. C. A. Schnepper and M. A. Stadtherr., Robust Process Simulation Using Interval Methods. Comput. Chem. Eng. 20, 187,1995.

11. A. C. Sun and W. D. Seider., Homotopy-Continuation Algorithm for Global Optimization In Recent Advances in Global Optimization; Floudas, C. A., Pardalos, P.M., Eds., Princeton University Press: Princeton, NJ, 1992.

12. C. D. Maranas and C. A. Floudas., Finding All Solutions to Nonlinearly Constrained Systems of Equations. J. Global Optim., 7, 143, 1995.

13. S. Kirkpatrick., C. D.Gelatt and M. P. Vecchi,, Optimization by Simulated Annealing. Sci Am, 220, 671, 1983.

14. J. H. Holland., Genetic Algorithms, Sci. Am., 267, 66, 1992.

15. A. Lucia and F. Yang,. Multivariable Terrain Methods. AIChE J., 49, 2553, 2003.

16. A. Lucia., P. A. DiMaggio, Depa and P. A Geometric Terrain Methodology for Global Optimization. J. Global Optim, 29, 297, 2004.

17. B. Carnahan., H. A. Luther and J. O. Wilkes, Applied Numerical Methods; Wiley: New York, 1969.

18. D. H. Kim and J. A.Lee, Robust Iterative Method of Computing Effectiveness Factors in Porous Catalysts. Chem. Eng. Sci., 59, 2253, 2004.

19. Y. Lin, J. A. Enszer, Stadtherr, M. A. Enclosing All Solutions of Two-Point Boundary value Problems for ODEs. Comput. Chem. Eng., 2007,

20. Angelo Lucia, R. Rajeswar and A.Gattupalli, Barrier-Terrain Methodology for Global Optimization, Ind. Eng. Chem. Res., 47, 2666-2680, 2008.

21. J. V. Villadsen and M. L. Michelsen., Solution of Differential Equations by Polynomial Approximation; Prentice Hall: New York, 1978.

22. A. Lucia., P. A. DiMaggio and P. A. Depa,, Geometric Terrain Methodology for Global Optimization. J. Global Optim., 29, 297, 2004.

23. P. B. Weisz and J. S.Hicks., The Behavior of Porous Catalyst Particles in View of Internal Mass and Heat Diffusion Effects. Chem. Eng. Sci., 17, 265, 1962.

24. G. Adomian,, Convergent series solution of nonlinear equations, J. Comp. App. Math., 11, 225-230, 1984.

25. Y. Q. Hasan and L. M. Zhu, L., Modified Adomian decomposition method for singular initial value problems in the second-order ordinary differential equations, Surveys in Mathematics and its Applications., 3, 183-193, 2008.

26. M. M. Hosseini, Adomian decomposition method with Chebyshev polynomials, Appl. Math. Comput., 175, 1685-1693, 2006.

27. A. M. Wazwaz and A reliable modification of Adomian decomposition method, Appl. Math Comput., 102, 77-86, 1999.

28. A. M. Wazwaz,, Analytical approximations and Pade approximations for Volterra's population model, Appl. Math. Comput., 100, 13-25, 1999.

29. A. M. Wazwaz,, A new method for solving singular initial value problems in the second-order ordinary differential equations, Appl. Math. Comput., 128, 45-57, 2002.

Conclusions and Future Enhancements

Chapter 6

6.1. Conclusions

In this book asymptotic methods such as Homotopy perturbation method, Homotopy analysis method and Adomain decomposition method were employed to obtain solution of various non-linear boundary value problems in bio-chemical systems. The influence of the parameter is discussed in detail. The validity of the obtained solutions is verified by the numerical results.

➢ Analytical expressions of concentrations inside the cationic glucose-sensitive membrane is obtained using, Homotopy analysis method.

➢ Time-dependent nonlinear reaction equations in immobilized enzyme systems were solved analytically and numerically. The closed analytical expressions of concentrations and current were obtained using Homotopy perturbation method.

➢ Approximate solution of non-linear boundary value problems in immobilized glucoamylase kinetics is evaluated using Adomain decomposition method, Homotopy analysis method and Homotopy perturbation method.

➢ The analytical expression of concentration and effectiveness factor of the reactant inside the catalyst pellets is derived using modified Adomain decomposition method.

6.2. Future Enhancements

The present investigation offers future enhancement on the following lines.

❖ The approach employed here to evaluate the concentration of oxygen, glucose, and gluconic acid for all values of parameters is extended for the non-steady state conditions.

❖ The Homotopy perturbation method can also be employed in obtaining current pertaining to membrane-based biosensor, amperometric biosensors and potentiometric biosensor.

❖ This method which is used to find the concentration and effectiveness factor in heterogeneous reaction kinetics can be extended to all reaction mechanics

❖ This anatical procedure can also be extended to find the solution of Poisson-Boltzmann equation (PBE), a three-dimensional second order nonlinear elliptic partial differential equation arising in biophysics, nuclear physics, semiconductor physics, population genetics and astrophysics. This problem has several interesting features impacting numerical algorithms,

6.1. Conclusions

In this book asymptotic methods such as Homotopy perturbation method, Homotopy analysis method and Adomain decomposition method were employed to obtain solution of various non-linear boundary value problems in bio-chemical systems. The influence of the parameter is discussed in detail. The validity of the obtained solutions is verified by the numerical results.

➢ Analytical expressions of concentrations inside the cationic glucose-sensitive membrane is obtained using, Homotopy analysis method.

➢ Time-dependent nonlinear reaction equations in immobilized enzyme systems were solved analytically and numerically. The closed analytical expressions of concentrations and current were obtained using Homotopy perturbation method.

➢ Approximate solution of non-linear boundary value problems in immobilized glucoamylase kinetics is evaluated using Adomain decomposition method, Homotopy analysis method and Homotopy perturbation method.

➢ The analytical expression of concentration and effectiveness factor of the reactant inside the catalyst pellets is derived using modified Adomain decomposition method.

6.2. Future Enhancements

The present investigation offers future enhancement on the following lines.

❖ The approach employed here to evaluate the concentration of oxygen, glucose, and gluconic acid for all values of parameters is extended for the non-steady state conditions.

❖ The Homotopy perturbation method can also be employed in obtaining current pertaining to membrane-based biosensor, amperometric biosensors and potentiometric biosensor.

❖ This method which is used to find the concentration and effectiveness factor in heterogeneous reaction kinetics can be extended to all reaction mechanics

❖ This anatical procedure can also be extended to find the solution of Poisson-Boltzmann equation (PBE), a three-dimensional second order nonlinear elliptic partial differential equation arising in biophysics, nuclear physics, semiconductor physics, population genetics and astrophysics. This problem has several interesting features impacting numerical algorithms, including discontinuous coefficients representing material interfaces, rapid nonlinearities, and three spatial dimensions.

7. Acknowledgement

We take this opportunity with much pleasure to thank all the people who have helped me through the course of my journey towards producing this book.

The authors are thankful to Shri J. Ramachandran, Chancellor, Col. and Dr. G. Thiruvasagam, Vice-Chancellor, Academy of Maritime Education and Training (AMET), Chennai, Tamil Nadu for the encouragement. we also extend my sincere thanks to the M. ***Jayaprakashvel***, Registrar, and Dr N Rajasekar, Director of Research, and all staff in the Mathematics Department, AMET University, Chennai for their help and motivation

We also extend my thanks to all the members of our family. Last but not least, I contribute my heartfelt thanks to one and all who bestowed their blessings directly and indirectly to shape my entire research works.

ABOUT THE AUTHORS

Dr. Lakshmanan Rajendran is a Professor and head at the Department of Mathematics, Academy of Maritime Education and Training (Deemed to be University), Chennai, India. He has published 120 papers in international/SCI journals and 100 papers in national journals. He has also written four books. He serves as a reviewer in many International Journals. He completed 6 research projects from various funding agencies in India. More than 35 students completed the Ph.D under his guidance. He visited Germany and Poland, under INSA fellowships.

Dr. R Swaminathan is a renowned academician specialising in Mathematics, who has dedicated his life and existence in the field Education. Under his tutelage and guidance, *thousands of students* have embarkedon successful career paths and carried forward his ethos of professionalism and excellence into their lives. He is a quintessential and staunch advocate on disseminating **QUALITY** education to the masses irrespective of gender, race or background. He is revered amongst his students; current or former and well-respected amongst his peers. His functionality is not limited to his teaching methodologies but also matched in his varying and multi-tasked roles as administrator, principal, secretary and syndicate member, to name a few. He currently serves as the Principal and Head of the Department of Mathematics *Vidhyaa Giri College* of *Arts and Science* in Puduvayal, Karaikudi and concurrently avails as syndicate member of Alagappa University. He has been credited in adopting new innovative practices not only in teaching modes but also in management style along with high decisional stances.

His vast experience totaling 35 years and counting has led him to Author Mathematics textbooks for State Universities and also for School Education. He is also the Recipient of the *Dr.S. Radhakrishnan State award for Best Teacher for the year* 2002-2003. In addition, he was also awarded the BOLT-BROAD-OUTLOOK-LEARNER, TEACHER award in 2003. TATA Consultancy Services honoured him by recognizing him with the “Education India’s Best Teacher” award in 2005.